BAREKENG: Journal of Mathematics and Its Applications
September 2026 Volume 20 Issue 3 Page 2259-2280
P-ISSN: 1978-7227 E-ISSN: 2615-3017
https://doi.org/10.30598/barekengvol20iss3pp2259-2280

MATHEMATICAL MODELLING AND OPTIMAL INTERVENTION STRATEGIES FOR MENINGITIS TRANSMISSION DYNAMICS

Ayodeji Sunday Afolabi [1*], **Abdulwahab Ridwan** [2], **Princess Chiamaka Uche** [3]

[1,2,3]*Department of Mathematical Sciences, The Federal University of Technology Akure, PMB 704, Nigeria*

*Corresponding author's e-mail: * **asafolabi@futa.edu.ng***

Article Info

Article History:

Received: 12th August 2025
Revised: 1st February 2026
Accepted: 10th March 2026
Available online: 8th April 2026

Keywords:

Basic Reproduction Number;
Chemoprophylaxis administration:
Mathematical modelling;
Meningitis;
Optimal control;
Sensitivity analysis;
Stability analysis.

ABSTRACT

Meningitis remains a major public health concern, particularly within the African meningitis belt, where recurrent outbreaks pose severe health and socio-economic challenges. The disease is transmitted through close contact and is driven by complex human-to-human dynamics. While vaccination campaigns and treatment programs are central to control efforts, limitations such as waning immunity and delayed case detection often reduce their long-term impact. In alignment with global health recommendations, integrated control approaches that combine prevention, vaccination, and timely treatment are increasingly being advocated. In this study, a novel deterministic nonlinear seven-compartmental model, SVECITR, is developed. The model's validity is confirmed through positivity and boundedness analyses, and key thresholds such as the DFE and the R_0, are derived using the next-generation matrix method. Stability analysis was also performed. The framework is extended into an optimal control problem using three time-dependent interventions: public health education, booster vaccine administration, and prophylactic chemoprophylaxis. Using Pontryagin's Maximum Principle, optimal strategies are obtained, and numerical techniques are employed to simulate various intervention scenarios. Our results reveal that while dual interventions moderately reduce disease prevalence, the combined application of all three control measures resulted in the most substantial decline in transmission. Cost-effectiveness analysis, which employs the Incremental Cost-Effectiveness Ratio (ICER), Average Cost-Effectiveness Ratio (ACER), and Infection Averted Ratio (IAR), shows that combining booster vaccination and prophylactic chemoprophylaxis emerges as the most cost-effective option. These findings suggest that, in resource-limited settings, public health authorities should prioritize booster vaccination and chemoprophylaxis administration to curb the spread of meningitis while optimizing the use of available resources.

How to cite this article:

A. S. Afolabi, A. Ridwan, and P. C. Uche, "MATHEMATICAL MODELLING AND OPTIMAL INTERVENTION STRATEGIES FOR MENINGITIS TRANSMISSION DYNAMICS", *BAREKENG: J. Math. & App.*, vol. 20, no. 3, pp. 2259-2280, Sep, 2026.

Journal homepage: *https://ojs3.unpatti.ac.id/index.php/barekeng/*
Journal e-mail: *barekeng.math@yahoo.com; barekeng.journal@mail.unpatti.ac.id*

Research Article · Open Access

1. INTRODUCTION

Meningitis, which is also known as Meningeal inflammation, is a deadly disease that affects the meninges and spinal cord [1]– [4]. This condition can be caused by a variety of pathogens and irritants. The primary causes include viruses, bacteria, fungi, parasites, protozoa, and, in some cases, chemical irritation, subarachnoid hemorrhage, and cancer [1], [5]– [7]. However, bacteria have been linked to the greatest global burden of meningitis cases to date [6], [8]. The pathogens that cause meningitis are transferred from one person to another by respiratory droplets in the air or saliva. Prolonged and intimate touch, like kissing, coughing, sneezing, or residing in close proximity to someone infected, increases the risk of infection. The incubation period typically lasts around four days but can range from two to ten days [9]. While bacterial meningitis may have initially spread from animals to humans, it is now commonly passed between individuals through contaminated surfaces, secretions, or airborne droplets. Factors like overcrowded living conditions, large gatherings, sharing utensils, and close interactions further facilitate its spread with symptoms such as high fever, severe headache, vomiting, and so on [10], [11]. As the illness progresses, it may lead to more serious complications such as convulsions, delirium, and even death. Management strategies for bacterial meningitis include preventive vaccination and curative treatment with antibiotics [12]– [14]. Various vaccines have been developed to help control meningitis, including the meningococcal A conjugate vaccine, C conjugate vaccine, tetravalent conjugate vaccines, as well as meningococcal polysaccharide vaccines [15], [16].

Each year, over 1.2 million cases of bacterial meningitis are recorded globally [17]. The disease shows variation in incidence and fatality rates depending on the region, pathogen, and age group affected. In 2025, the WHO reported that for the year 2024, there were approximately 2.5 million reported cases globally, resulting in 250,000 deaths [3]. Africa, particularly sub-Saharan Africa, bears the greatest burden of bacterial meningitis. This region hosts the so-called meningitis belt [11], [18]. Each year, up to 1.2 million people are affected, with approximately 135,000 deaths reported. Nigeria, as a key country within the meningitis belt, is particularly vulnerable to recurrent outbreaks. Historical records show a series of epidemics, including three consecutive years ending in 2024, primarily due to vaccine shortages [3], [19], [20].

In order to properly comprehend the principles governing the dynamics of disease transmission, mathematical models are essential. Most often, non-linear deterministic compartmental models are employed to capture the complex interactions among various population groups and to simulate the progression of infectious diseases over time [1]– [40]. For instance, [11] employed non-linear compartmental models to investigate the transmission trend of meningitis and analysed the conditions for the stability of the model. [32] investigated the dynamics of meningococcal meningitis in sub-Saharan Africa, causing significant mortality. Using mathematical modelling, the study identified key factors influencing the disease's spread.

A novel two-strain SVCIR compartmental model that identified the transmission probability, β, as the most influential parameter for both strains 1 and 2 was presented. The findings showed that if at least 25% of people are immune to bacterial meningitis, the illness will not spread throughout the population. However, the model did not include the asymptomatic and treated compartments [1]. [17] highlighted carriers as key drivers of transmission. An optimal control strategy combining vaccination, treatment, and public health education was found to be the most effective in minimizing infection and control costs, especially in Sub-Saharan Africa. [9] investigated the impact of influenza infection on the transmission dynamics of meningitis using a nonlinear mathematical model. The stability analysis and numerical simulations revealed that the basic reproduction number varied with contact and quarantine rates. Higher quarantine and recovery rates led to increased recovery in the population, offering insights into effective control of co-infections. [4] employed a Suspected–Exposed–Infected–Recovered (SEIR) compartmental model to investigate the dynamics of meningitis transmission. The model was analysed for the stability of its disease-free and endemic equilibrium points using Descartes' Rule of Signs. [7] developed a mathematical model for meningococcal meningitis incorporating incidence-dependent self-protection measures and information-based vaccination. Using optimal control theory, the research demonstrated that combining preventive education, vaccination, and treatment effectively reduces the disease incidence. [8] formulated a deterministic compartmental model for bacterial meningitis incorporating a drug-resistant class. [10] presented a model for the investigation of the impact of counterfeit and non-counterfeit drugs on the treatment of bacterial meningitis. The study highlighted that administering counterfeit drugs can increase mortality rates, especially in regions with poor regulatory oversight. Numerical simulations have demonstrated the heightened severity of illness in areas prone to counterfeit medications, emphasizing the importance of safeguarding drug supply chains through coordinated stakeholder efforts. [6] presented a deterministic

compartmental model of bacterial meningitis using the SVCITR approach. The model, comprising seven epidemiological compartments, was analysed for its invariant region, positivity, and equilibrium stability.

This research addresses a critical gap in existing meningitis modeling studies, where the combined optimization of multiple intervention strategies under cost and resource constraints remains insufficiently explored. Consequently, this research presents a strategically oriented, multi-intervention optimal control model designed to answer practical policy questions about which combination of interventions provides the best balance of epidemiological impact and economic efficiency for endemic regions with limited resources.

2. RESEARCH METHODS

A nonlinear deterministic seven-compartment dynamic model is developed for the spread and control of meningitis. The population is categorized into seven compartments: Susceptible (S), Vaccinated (V), Exposed (E), Carrier (C), Infected (I), Treated (T), and Recovered (R). Thus, the total population at time t is given by $N = S + V + E + C + I + T + R$.

The force of infection $\lambda = \beta\,(\tau\, E + \upsilon\, C + I)$, where β is the effective transmission probability, τ and υ are the modification parameters for the exposed and carrier populations, respectively. λ is constructed to account for the differential infectious contributions of exposed and carrier individuals relative to fully infectious cases, reflecting their reduced but non-negligible roles in the disease transmission. The proposed model for the transmission dynamics of Meningitis and definitions of the model parameters are given below:

$$\begin{cases} \dfrac{dS}{dt} = \alpha + \omega V - \kappa S - \lambda S - \mu S, \\ \dfrac{dV}{dt} = \kappa S - (1-\epsilon_1)\lambda V - \omega V - \mu V, \\ \dfrac{dE}{dt} = \lambda S + (1-\epsilon_1)\lambda V - \sigma_1 E - \sigma_2 E - \sigma_3 E - \mu E, \\ \dfrac{dC}{dt} = \sigma_1 E - \gamma C - \mu C, \\ \dfrac{dI}{dt} = \sigma_2 E + \gamma\rho C - \eta_1 I - \delta I - \mu I, \\ \dfrac{dT}{dt} = \eta_1\epsilon_2 I - \eta_2 T - \delta T - \mu T, \\ \dfrac{dR}{dt} = \sigma_3 E + \gamma(1-\rho)C + \eta_1(1-\epsilon_2)I + \eta_2 T - \mu R \end{cases} \tag{1}$$

With the initial conditions $S(0) > 0, V(0) \geq 0, E(0) \geq 0, C(0) \geq 0, I(0) > 0, T(0) > 0,$ and $R(0) > 0$.

Table 1. Description of the Model Parameters

Parameters	Description	Values	Source
α	Rate of entry	0.0413	[6]
ω	Vaccine waning rate	0.02	[26]
μ	Natural death rate	0.00068	[1]
κ	Vaccination rate	0.6	[1]
σ_1	Transition rate from the exposed population to the carrier population	0.6	[1]
σ_2	Transition rate from the exposed population to the infected population	0.0016	[41]
σ_3	Recovery rate of the exposed population by natural immunity	0.25	Assumed
γ	Recovery rate of the carrier population by natural immunity	0.37384	[7]
ρ	Proportion of carriers progressing to the infectious stage	0.00005	Assumed
δ	Disease-induced death rate	0.13	[6]
ϵ_1	Vaccination efficacy	0.85	[1]
ϵ_2	Drug efficacy	0.85	[1]
η_1	Transition rate from infected to treated population	0.1	Assumed
η_2	Recovery rate of treated individuals	0.08	Assumed

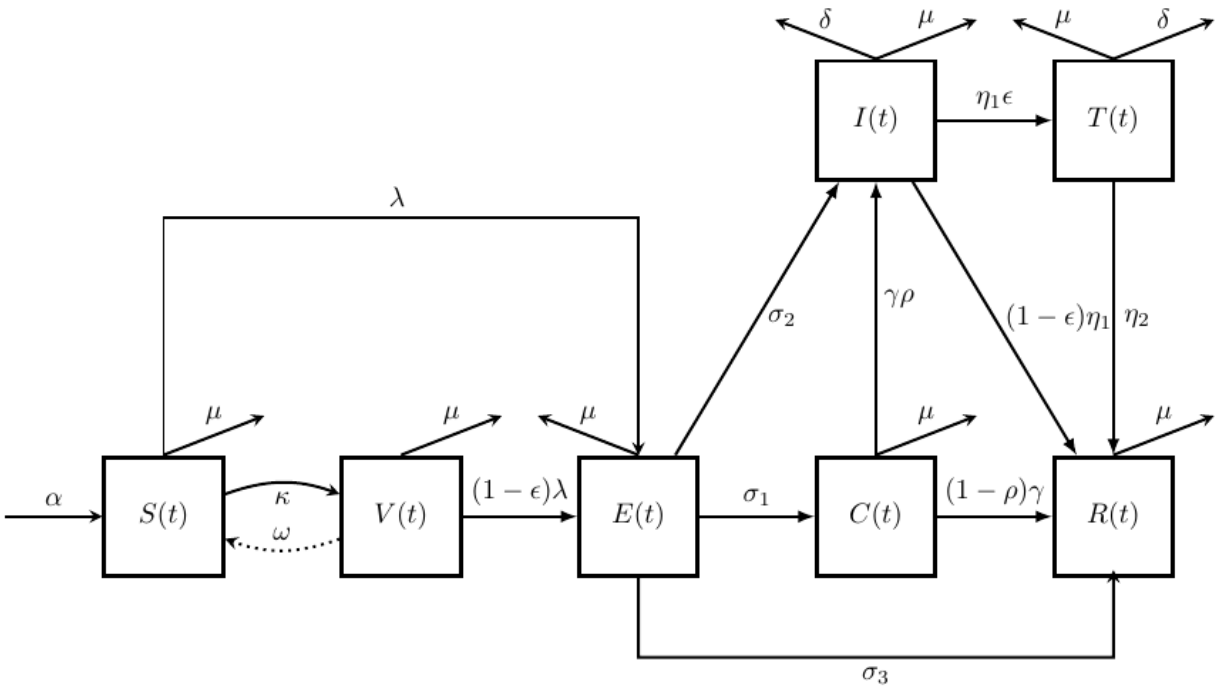

Figure 1. The Flowchart of the Proposed Model

3. RESULTS AND DISCUSSION

In this section, the model analysis of the proposed meningitis model is conducted. These include the invariant region, positivity of the solutions, and the disease-free equilibrium point (DFE).

Theorem 1. *The model 1 has a region defined by the set* $\Omega = \left\{(S+V+E+C+I+T+R) \in R_+^7 : N \leq \frac{\alpha}{\mu}\right\}$.

Proof. The total population is defined as $N = S+V+E+C+I+T+R$. Thus,

$$\frac{dN}{dt} = \frac{dS}{dt} + \frac{dV}{dt} + \frac{dE}{dt} + \frac{dC}{dt} + \frac{dI}{dt} + \frac{dT}{dt} + \frac{dR}{dt}. \tag{2}$$

Hence,

$$\frac{dN}{dt} \leq \alpha - \mu N \tag{3}$$

Thus, $N \in \left[0, \frac{\alpha}{\mu}\right]$. Therefore, the invariant region that contains the model 1 solutions is given by $\Omega = \left[(S,V,E,C,I,T,R) \in R_+^7 : N \leq \frac{\alpha}{\mu}\right]$ indicating that the region containing the model equation solutions is positively invariant and that model Eq. (1) is mathematically and biologically well-posed. ■

Theorem 2. *Let* $\Omega(t) = S,V,E,C,I,T,R \in R_+^7 : S_0 > 0, V_0 > 0, E_0 > 0, C_0 > 0, I_0 > 0, T_0 > 0$ *and* $R_0 > 0$ *then the solutions of* (S,V,E,C,I,T,R) *are positive for* $t \geq 0$.

Proof. Consider the first equation of the model in Eq. (1),

$$\frac{dS}{dt} = \alpha + \omega V - \kappa S - \lambda S - \mu S\,. \tag{4}$$

This implies:

$$\frac{dS(t)}{dt} \geq -(\kappa + \lambda + \mu)S. \tag{5}$$

Integrating,

$$S \geq S(0)e^{-(\mu+\kappa)t-\int_0^t \lambda(\phi)\,d\phi} \geq 0, \quad \text{for } t \geq 0, \tag{6}$$

where $\lambda(\eta) = \beta(\nu C + \tau E + I)$. In a similar approach, $V \geq 0, E \geq 0, C \geq 0, I \geq 0, T \geq 0, R \geq 0 \;\; i.e$

Hence, all variables of the model are positive for all $t \geq 0$

$$\begin{cases} V \geq V(0)e^{-\left((\omega+\mu)t+(1-\epsilon_1)\int_0^t \lambda(\phi)d\phi\right)} \geq 0, \\ E \geq E(0)e^{-((\sigma_1+\sigma_2+\sigma_3+\mu)t)} \geq 0, \\ C \geq C(0)e^{-((\gamma+\mu)t)} \geq 0, \\ I \geq I(0)e^{-((\eta_1+\delta+\mu)t)} \geq 0, \\ T \geq T(0)e^{-((\eta_2+\delta+\mu)t)} \geq 0, \\ R \geq R(0)e^{-(\mu t)} \geq 0. \end{cases} \tag{7}$$

3.1 The Equilibrium Points

3.1.1 The Disease-Free Equilibrium Point (DFE)

At DFE, there are no infections or recovery of the disease. Therefore, $E(t) = C(t) = I(t) = 0$ at the DFE. As a result, the DFE is given by

$$\mathcal{E}^0 = \left(S^0 = \frac{\alpha(\omega+\mu)}{\mu(\kappa+\omega+\mu)}, V^0 = \frac{\alpha\kappa}{\mu(\kappa+\omega+\mu)}, E^0 = 0, C^0 = 0, I^0 = 0, T^0 = 0, R^0 = 0\right). \tag{8}$$

Satisfying $\frac{dS}{dt} = \frac{dV}{dt} = \frac{dE}{dt} = \frac{dC}{dt} = \frac{dI}{dt} = \frac{dT}{dt} = \frac{dR}{dt} = 0.$

3.1.2 The Endemic Equilibrium Point (EEP)

The EEP is a positive steady state solution when the disease is expected to persist within the observed population. The EEP is obtained by equating each of the equations of the model in Eq. (1) to 0, i.e.,

$$\frac{dS}{dt} = \frac{dV}{dt} = \frac{dE}{dt} = \frac{dC}{dt} = \frac{dI}{dt} = \frac{dT}{dt} = \frac{dR}{dt} = 0$$

Thus, the EEP is expressed as:

$$\begin{aligned}
S^* &= \frac{\alpha\left((1-\epsilon_1)\lambda^* + k_2\right)}{(k_1+\lambda^*)((1-\epsilon_1)\lambda^* + k_2 - \kappa\omega}, \\
V^* &= \frac{\alpha\kappa}{(k_1+\lambda^*)((1-\epsilon_1)\lambda^* + k_2 - \kappa\omega}, \\
E^* &= \frac{\alpha\lambda^*((1-\epsilon_1)(\lambda^*+\kappa)+k_2)}{\kappa((k_1+\lambda^*)((1-\epsilon_1)\lambda^* + k_2 - \kappa\omega))}, \\
C^* &= \frac{\sigma_1 E^*}{k_4}, \\
I^* &= \frac{(\sigma_2 k_4 - \gamma\rho\sigma_1)E^*}{k_4 k_5}, \\
T^* &= \frac{(\sigma_2 k_4 - \gamma\rho\sigma_1)E^*}{k_4 k_5 k_6}, \\
R^* &= \frac{(k_5 k_6(\sigma_3 k_4 + \gamma\sigma_1(1-\rho)) + (\eta_1(1-\epsilon_2)k_6 + \eta_1\eta_2\epsilon_2)(\sigma_2 k_4 - \gamma\rho\sigma_1))E^*}{\mu k_4 k_5 k_6},
\end{aligned}$$

where $k_1 = (\kappa+\mu), \;\; k_2 = (\omega+\mu), \;\; k_3 = (\sigma_1+\sigma_2+\sigma_3+\mu), \;\; k_4 = (\gamma+\mu), k_5 = (\eta_1+\delta+\mu), \;\; k_6 = (\eta_2+\delta+\mu), \lambda^* = \beta(\tau E^* + \nu C^* + I^*)$ and λ^* represents the force of infection at EEP.

3.2 Stability Analysis of the DFE

3.2.1 The Basic Reproduction Number

The spectral radius of the matrix FV^{-1} obtained from the model in Eq. (1) is used to calculate the $\mathbb{R}_0$ in accordance with the next-generation matrix approach. Thus, by constructing F, the Jacobian matrix representing the rates of new infections, and V, the Jacobian matrix representing the rates of transfer between infected compartments (excluding new infections), and then obtaining V^{-1}, the $\mathbb{R}_0$ at the DFE is defined as:

$$\mathbb{R}_0 = \frac{\beta\alpha\left(\left((1-\epsilon_1)\kappa + k_2\right)\left(\sigma_1(\gamma\rho + \nu k_5) + k_4(\tau k_5 + \sigma_2)\right)\right)}{\mu k_3 k_4 k_5 (k_2 + \kappa)}. \tag{9}$$

Theorem 3. *The DFE is locally asymptotically stable (LAS) when* $\mathbb{R}_0 < 1$, *and it becomes unstable whenever* $\mathbb{R}_0 > 1$.

Proof. In order to prove Theorem 3, the method outlined in [1], [42], [43] is adopted. The Jacobian matrix of the model in Eq. (1) at the DFE, denoted as $J(\mathcal{E}^0)$ is expressed as:

$$J(\mathcal{E}^0) = \begin{bmatrix} -\kappa-\mu & \omega & -\frac{\beta\tau\alpha k_2}{\mu(k_2+\kappa)} & -\frac{\beta\nu\alpha k_2}{\mu(k_2+\kappa)} & -\frac{\beta\alpha k_2}{\mu(k_2+\kappa)} & 0 & 0 \\ \kappa & -k_2 & -\frac{(1-\epsilon_1)\beta\tau\alpha\kappa}{\mu(k_2+\kappa)} & -\frac{(1-\epsilon_1)\beta\nu\alpha\kappa}{\mu(k_2+\kappa)} & -\frac{(1-\epsilon_1)\beta\alpha\kappa}{\mu(k_2+\kappa)} & 0 & 0 \\ 0 & 0 & \frac{\beta\tau\alpha k_2}{\mu(k_2+\kappa)} + \frac{(1-\epsilon_1)\beta\nu\alpha\kappa}{\mu(k_2+\kappa)} - k_3 & \frac{\beta\nu\alpha k_2}{\mu(k_2+\kappa)} + \frac{(1-\epsilon_1)\beta\tau\alpha\kappa}{\mu(k_2+\kappa)} & \frac{\beta\alpha k_2}{\mu(k_2+\kappa)} + \frac{(1-\epsilon_1)\beta\alpha\kappa}{\mu(k_2+\kappa)} & 0 & 0 \\ 0 & 0 & \sigma_1 & -k_4 & 0 & 0 & 0 \\ 0 & 0 & \sigma_2 & \gamma\rho & -k_5 & 0 & 0 \\ 0 & 0 & 0 & 0 & \epsilon_2\eta_1 & -k_6 & 0 \\ 0 & 0 & \sigma_3 & \gamma(1-\rho) & \eta_1(1-\epsilon_2) & \eta_2 & -\mu \end{bmatrix} \tag{10}$$

The characteristic polynomial, $P(\lambda^*)$, corresponding to Eq. (10) is expressed as:

$$P(\lambda^*) = |J(\mathcal{E}^0) - \lambda^* \mathbb{I}_7|$$

The eigenvalues of $J(\mathcal{E}^0)$ are determined by solving $P(\lambda^*) = 0$ and thus, the first two eigenvalues are:

$$\lambda_i^* = \begin{pmatrix} -\mu, \\ -\delta - \mu - \eta_2 \end{pmatrix}. \tag{11}$$

The remaining eigenvalues of the reduced system can be obtained from:

$$\mathcal{J}(\mathcal{E}^1) = \begin{bmatrix} -\kappa-\mu & \omega & -\frac{\beta\tau\alpha k_2}{\mu(k_2+\kappa)} & -\frac{\beta\nu\alpha k_2}{\mu(k_2+\kappa)} & -\frac{\beta\alpha k_2}{\mu(k_2+\kappa)} \\ \kappa & k_2 & -\frac{(1-\epsilon_1)\beta\tau\alpha\kappa}{\mu(k_2+\kappa)} & -\frac{(1-\epsilon_1)\beta\nu\alpha\kappa}{\mu(k_2+\kappa)} & -\frac{(1-\epsilon_1)\beta\alpha\kappa}{\mu(k_2+\kappa)} \\ 0 & 0 & \frac{\beta\tau\alpha k_2}{\mu(k_2+\kappa)} + \frac{(1-\epsilon_1)\beta\nu\alpha\kappa}{\mu(k_2+\kappa)} - k_3 & \frac{\beta\nu\alpha k_2}{\mu(k_2+\kappa)} + \frac{(1-\epsilon_1)\beta\tau\alpha\kappa}{\mu(k_2+\kappa)} & \frac{\beta\alpha k_2}{\mu(k_2+\kappa)} + \frac{(1-\epsilon_1)\beta\alpha\kappa}{\mu(k_2+\kappa)} \\ 0 & 0 & \sigma_1 & -k_4 & 0 \\ 0 & 0 & \sigma_2 & \gamma\rho & -k_5 \end{bmatrix} \tag{12}$$

According to the Routh-Hurwitz standard, the matrix $\mathcal{J}(\mathcal{E}^0)$ will possess both negative and real eigenvalues if $Tr(\mathcal{J}(\mathcal{E}^0)) < 0$ and $\det(\mathcal{J}(\mathcal{E}^0)) > 0$.

From Eq. (12)

$$Det(\mathcal{J}) = (1-\mathbb{R}_0)\left(k_3 k_4 k_5\left(\kappa\omega + k_2(\kappa+\mu)\right)\right) > 0 \text{ if } \mathbb{R}_0 < 1. \tag{13}$$

Since the first two eigenvalues of the associated Jacobian matrix are negative, and the trace and determinant of the reduced matrix also satisfy the Routh-Hurwitz criteria, this implies that the disease-free equilibrium (DFE) is LAS. ■

3.2.2 Global Asymptotic Stability Analysis (GAS)

The global stability of the DFE within $\Omega \in \mathbb{R}_+^7$ is obtained by denoting the system in Eq. (1) by

$$\begin{cases} \dfrac{dX}{dt} = F(X,Y), \\ \dfrac{dY}{dt} = G(X,Y), \quad G(X,0) = 0. \end{cases} \tag{14}$$

where $X = (S, V, R)$ denotes the uninfected sub-populations and $Y = (E, C, I, T)$ comprises the infected sub-populations. The DFE is said to GAS if $R_0 < 1$ and provided that the following two conditions are satisfied:

$$\text{Condition I: } \frac{dX}{dt} = F(X,0), X^* = (S^0, V^0, E^0, C^0, I^0, T^0, R^0) \text{is GAS and,} \tag{15}$$

$$\text{Condition II: } G(X,Y) = BY - G^*(X,Y), G^*(X,Y) \geq 0 \ \forall \ (X,Y) \in \mathbb{R}_+^7, \tag{16}$$

where $B = D_Y G(X^*, 0)$, and $\mathbb{R}_+^7$ denotes the positively invariant region of the model system.

Theorem 4. *The point* $\left(S^0 = \frac{\alpha(\omega+\mu)}{\mu(\kappa+\omega+\mu)},\ V^0 = \frac{\alpha\kappa}{\mu(\kappa+\omega+\mu)},\ E^0 = 0,\ C^0 = 0,\ I^0 = 0,\ T^0 = 0,\ R^0 = 0\right) \in \mathbb{R}_+^7$ *is GAS for the model in Eq. (1), if* $\mathbb{R}_0 < 1$ *and conditions I and II are held.*

Proof. If all the infected compartments are set to zero**,** then the corresponding disease-free state is given by

$$F(X(t), 0) = \begin{pmatrix} \alpha + \omega V - \kappa S + \mu S \\ \kappa S - (\omega + \mu)V \\ -\mu R \end{pmatrix}, \tag{17}$$

$$\mathcal{E}^0 = \left(S^0 = \frac{\alpha(\omega+\mu)}{\mu(\kappa+\omega+\mu)}, V^0 = \frac{\alpha\kappa}{\mu(\kappa+\omega+\mu)}, E^0 = 0, C^0 = 0, I^0 = 0, T^0 = 0, R^0 = 0\right).$$

To verify the equation above, the first equation of the system, Eq. (1), implies that

$$\frac{dS(t)}{dt} = \alpha + \omega V - (\kappa + \mu)S, \tag{18}$$

then solving the above equation using the method of integrating factor:

$$\frac{dS(t)}{dt} + (\kappa + \mu)S(t) = \alpha + \omega V. \tag{19}$$

The integrating factor is:

$$IF = e^{(\kappa+\mu)t} \tag{20}$$

Multiplying both sides by $e^{(\kappa+\mu)t}$, yields:

$$e^{(\kappa+\mu)t}\frac{dS(t)}{dt} + (\kappa + \mu)e^{(\kappa+\mu)t}S(t) = \alpha e^{(\kappa+\mu)t} + \omega V e^{(\kappa+\mu)t} \tag{21}$$

Now, solving for $S(t)$:

$$S(t)e^{(\kappa+\mu)t} = \frac{\alpha}{(\kappa+\mu)}e^{(\kappa+\mu)t} + \omega \int V e^{(\kappa+\mu)t}, \tag{22}$$

$$\int V e^{(\kappa+\mu)t} = \frac{V e^{(\kappa+\mu)t}}{(\kappa+\mu)} - \int \frac{V' e^{(\kappa+\mu)t}}{(\kappa+\mu)}. \tag{23}$$

Thus, Eq. (22) becomes:

$$S(t) = \frac{\alpha}{(\kappa+\mu)} + \frac{\omega V}{(\kappa+\mu)} - \frac{\omega}{(\kappa+\mu)e^{(\kappa+\mu)t}} \int \frac{V' e^{(\kappa+\mu)t}}{(\kappa+\mu)} \tag{24}$$

As $t \to \infty$, $S = \frac{\alpha+\omega V}{(\kappa+\mu)}$. Similarly,

$$\frac{dV(t)}{dt} = \kappa S - (\omega + \mu)V, \tag{25}$$

since $S = \frac{\alpha+\omega V}{(\kappa+\mu)}$, this implies that

$$\frac{dV(t)}{dt} = \frac{\kappa\alpha}{\kappa+\mu} - \left(\frac{(\omega+\mu)(\omega+\mu) - \kappa\omega}{(\omega+\mu)}\right)V \tag{26}$$

Solving for V using the integrating factor mentioned in the previous steps, we obtain $V = \frac{\alpha\kappa}{\mu(\kappa+\omega+\mu)}$ as $t \to \infty$. Thus, X^* is GAS for the system $\frac{dX}{dt} = F(X, 0)$. Hence, the first condition is fulfilled. Next, it follows that $\frac{dY(t)}{dt} = G(X(t), Y(t))$ for the system in Eq. (1),

$$G(X,Y) = \begin{pmatrix} \lambda S + (1-\epsilon_1)\lambda V - \sigma_1 E - \sigma_2 E - \sigma_3 E - \mu E \\ \sigma_1 E - \gamma C - \mu C \\ \sigma_2 E + \gamma\rho C - \eta_1 I - \delta I - \mu I \\ \eta_1\epsilon_2 I - \eta_2 T - \delta T - \mu T \end{pmatrix}, \tag{27}$$

where B is given as

$$B = \begin{pmatrix} \beta\tau S + (1-\epsilon_1)\beta\tau V - (\sigma_1+\sigma_2+\sigma_3+\mu) & \beta\nu S + (1-\epsilon_1)\beta\nu V & \beta S + (1-\epsilon)\beta V & 0 \\ \sigma_1 & -(\gamma+\mu) & 0 & 0 \\ \sigma_2 & \gamma\rho & -(\eta_1+\delta+\mu) & 0 \\ 0 & 0 & \eta_1\epsilon_2 & -(\eta_2+\delta+\mu) \end{pmatrix}, \tag{28}$$

and

$$B \cdot Y = \begin{pmatrix} [\beta\tau S + (1-\epsilon_1)\beta\tau V - (\sigma_1+\sigma_2+\sigma_3+\mu)]E + [\beta\nu S + (1-\epsilon_1)\beta\nu V]C + [\beta S + (1-\epsilon)\beta V]I \\ \sigma_1 E - (\gamma+\mu)C \\ \sigma_2 E + \gamma\rho C - (\eta_1+\delta+\mu)I \\ \eta_1\epsilon_2 I - (\eta_2+\delta+\mu)T \end{pmatrix}. \tag{29}$$

Recall from Condition II above that $G(X,Y) = BY - G^*(X,Y)$. This implies that

$$G^*(X(t), Y(t)) = \begin{pmatrix} 0 \\ 0 \\ 0 \\ 0 \end{pmatrix}. \tag{30}$$

Clearly $G^*(X,Y) \geq 0 \ \forall \ (X,Y) \in \mathbb{R}_+^7$. Hence, the DFE, as denoted, is GAS. ■

3.3 Sensitivity Analysis

The sensitivity index provides insight into how small changes in parameter values influence $\mathbb{R}_0$, helping to identify key factors affecting the disease transmission dynamics Ψ [7], [13], [44]– [46].

Definition 1. The normalized forward sensitivity index of $\mathbb{R}_0$ relative to a parameter Ψ according to [5], [26] is expressed as

$$S_\Psi^{\mathbb{R}_0} = \frac{\partial \mathbb{R}_0}{\partial \Psi} \times \frac{\Psi}{\mathbb{R}_0}. \tag{31}$$

Eq. (31) is employed to derive the sensitivity index (SI) of each parameter in $\mathbb{R}_0$. For instance, the SI of $\mathbb{R}_0$ with respect to τ is given by

$$S_\tau^{\mathbb{R}_0} = \frac{\partial \mathbb{R}_0}{\partial \tau} \times \frac{\tau}{\mathbb{R}_0} \approx 0.10326.$$

Using Eq. (31), the sensitivity indices for each parameter of $\mathbb{R}_0$ was calculated. Table 2 contains the parameter values, showing both the sign and numerical magnitude of each sensitivity index.

Table 2 shows that SI is positive for the parameters α, β, ν, ρ, τ, and σ_1, whereas it is negative for δ, κ, μ, η_1, γ_1, σ_2, and σ_3.

Table 2. Model Parameter Values

Parameters	Values	Parameters	Values	Parameters	Values
δ	-0.35755	ρ	0.89362	α_1	0.15457
κ	-0.01178	τ	0.10326	α_2	0.00016
η	-1.12614	η_1	-0.46482	α_3	0.25799
μ	0.00286	γ_1	0.06355		

From Table 2, it is evident that the parameters with the highest absolute sensitivity indices are η (1.12614), and ρ (0.89362). These parameters are important in determining the spread of the disease. Thus, implementing control measures to reduce the transmission probability from carriers (ρ) or implementing measures to reduce the effects of η could be effective in controlling disease transmission.

3.4 Optimal Control Problem (OCP)

The meningitis dynamic system presented in the model in Eq. (1) is extended into an OCP by incorporating three time-dependent control variables $u_i(t)$, for $i = 1,2,3$, where $u_1(t)$ is public health education campaigns, $u_2(t)$ is booster vaccine administration, and $u_3(t)$ is prophylactic chemoprophylaxis administration.

All three of the control variables are described below:

1. The control function $0 \le u_1(t) \le 1$ represents public health education campaigns. These include awareness creation on personal hygiene, early symptom reporting, avoidance of overcrowded places, and general community sensitization to prevent the spread of meningitis. The effect of $u_1(t)$ is to decrease the probability of the disease transmission, thereby modifying the force of infection to $P_\lambda^c = (1 - u_1(t))\lambda S(t)$.
2. The control function $0 \le u_2(t) \le 1$ represents booster vaccination against meningitis. Since immunity conferred by childhood vaccination wanes over time, booster doses are administered to maintain long-term protection. The effect of $u_2(t)$ is to reduce the rate at which vaccinated individuals move to the exposed class, and it is given by $P_{\epsilon\lambda}^c = u_2(t)(1 - \epsilon)\lambda V(t)$.
3. The control function $0 \le u_3(t) \le 1$ represents prophylactic chemoprophylaxis administration. This involves administering preventive antibiotics to individuals who have been exposed to meningitis, as well as those who are carriers of the disease, especially close contacts of confirmed cases. The goal is to prevent the progression from exposure and carriage to infectiousness. In the presence of $u_3(t)$, the progression from $E(t)$ and $C(t)$ to the infectious class is modified as $P_{\sigma_2}^c = (1 - u_3(t))\sigma_2 C(t)$ and $P_\gamma^c = (1 - u_3(t))\gamma A(t)$, respectively.

$$\begin{cases} \dfrac{dS}{dt} = \alpha + \omega V - \kappa S - \big(1 - u_1(t)\big)\lambda S - \mu S, \\ \dfrac{dV}{dt} = \kappa S - u_2(1 - \epsilon_1)\lambda V - \omega V - \mu V, \\ \dfrac{dE}{dt} = \big(1 - u_1(t)\big)\lambda S + u_2(1 - \epsilon_1)\lambda V - \sigma_1 E - \big(1 - u_3(t)\big)\sigma_2 E - \sigma_3 E - \mu E, \\ \dfrac{dC}{dt} = \sigma_1 E - \big(1 - u_3(t)\big)\gamma C - \mu C, \\ \dfrac{dI}{dt} = \big(1 - u_3(t)\big)\sigma_2 E + \big(1 - u_3(t)\big)\gamma\rho C - \eta_1 I - \delta I - \mu I, \\ \dfrac{dT}{dt} = \eta_1\epsilon_2 I - \eta_2 T - \delta T - \mu T, \\ \dfrac{dR}{dt} = \sigma_3 E + \big(1 - u_3(t)\big)\gamma(1 - \rho)C + \eta_1(1 - \epsilon_2)I + \eta_2 T - \mu R \end{cases} \tag{32}$$

Our goal is to examine the efforts required to control meningitis by minimizing the number of exposed E, carriers C and infectious individuals I, while also minimizing the cost associated with implementing the control strategies u_1, u_2, u_3. Accordingly, the objective functional is defined as:

$$J(u_1, u_2, u_3) = \int_0^{t_f} \left(\kappa_1 E + \kappa_2 C + \kappa_3 I + \frac{1}{2}\sum_{i=1}^{3} \xi_i u_i^2 \right) dt, \tag{33}$$

subject to the control system given in Eq. (32). Here, t_f denotes the last time for the implementation of the control strategies, and $\kappa_i > 0$, for $i = 1,2,3$, are weight constants associated with the exposed, carrier, and infected individuals, respectively. The terms $\frac{1}{2}\xi_i u_i^2(t)$, for $i = 1,2,3$, represent the costs associated with applying the respective control measures.

The primary objective is to determine the optimal control functions u_1^*, u_2^*, and u_3^* such that

$$J(u_1^*, u_2^*, u_3^*,) = \min_{\Phi} J(u_1, xi_2, xi_3), \tag{34}$$

where $\Phi = \{u_i : u_i(t) \in [0,1],\ 0 \le t \le t_f,\ i = 1,2,3\}$ are Lebesgue measurable functions.

Next, the existence of an optimal control problem is established. To derive the optimal solution, the Hamiltonian associated with the optimal control problem is formulated as

$$\mathcal{H} = \mathcal{L}(x, u, t) + \sum_{j=1}^{7} \lambda_j \cdot \dot{X}_j(t), \tag{35}$$

where $\dot{X}_j(t)$ denotes the derivatives of the state variables with respect to time.

Where $\mathcal{L}(x, u, t)$, the Lagrangian of the OCP, is defined as follows:

$$\mathcal{L}(x, u, t) = (\kappa_1 E + \kappa_2 C + \kappa_3 I) + \frac{1}{2}\sum_{i=1}^{3} \xi_i u_i^2(t). \tag{36}$$

Then, the results in the theorem below establish the existence of an optimal control, and with the method of Pontryagin's maximum principle as used and explained in [22], [47], [48], and [49].

Theorem 5. *The optimal control problem defined by Eqs. (32) and (33) along with the initial conditions at $t = 0$ is an optimal solution if there exists a control triple $(u_1^*, u_2^*, u_3^*) \in \Phi$ such that*

$$J(u_1^*, u_2^*, u_3^*) = \min_{(u_1, u_2, u_3) \in \Phi} J(u_1, u_2, u_3),$$

then an optimal control exists.

Proof. To establish the results presented in Theorem 5, the following properties are demonstrated:

1. The control set is both convex and closed.
   Since all of its limit points are contained in Φ, it follows that Φ is closed. Moreover, let $\lambda \in [0,1]$, and consider any two arbitrary elements $p, q \in \Phi$, where $p = (p_1, p_2, p_3)$ and $q = (q_1, q_2, q_3)$. Then, for each $j = 1,2,3$:

   $$\lambda p_j + (1 - \lambda) q_j \in \Phi.$$

   This confirms that Φ is convex.

2. The model in Eq. (32) has non-negative and bounded solutions.
   Given the initial conditions $\mathcal{W} \ge 0$, with $\mathcal{W} = (S, V, C, A, I, T, R) \in \mathbb{R}_+^7$, the optimal control problem is a non-negative and bounded solution, with control functions that are Lebesgue measurable. The system defined in Eq. (32) can thus be represented in the compact form:

   $$\frac{d\mathcal{W}}{dt} = \mathcal{D}(\psi)\mathcal{W} + \mathcal{G}(\psi, \mathcal{W}), \tag{37}$$

   where $\psi = (u_1, u_2, u_3)$ represents the control vector. The matrix $\mathcal{D}(\psi)$ is defined as:

$$\begin{pmatrix} -\kappa - \mu & \omega & 0 & 0 & 0 & 0 & 0 \\ \kappa & -\omega - \mu & 0 & 0 & 0 & 0 & 0 \\ 0 & 0 & -\sigma_1 - (1-u_3)\sigma_2 - \sigma_3 - \mu & 0 & 0 & 0 & 0 \\ 0 & 0 & \sigma_1 & -(1-u_3)\gamma - \mu & 0 & 0 & 0 \\ 0 & 0 & (1-u_3)\sigma_2 & (1-u_3)\gamma\rho & -\eta_1 - \delta - \mu & 0 & 0 \\ 0 & 0 & 0 & 0 & \eta_1\epsilon_2 & -\eta_2 - \delta - \mu & 0 \\ 0 & 0 & \sigma_3 & (1-u_3)\gamma(1-\rho) & \eta_1(1-\epsilon_2) & \eta_2 & -\mu \end{pmatrix} \tag{38}$$

   and

$$\mathcal{G}(\psi,\mathcal{W})=\begin{pmatrix}\alpha-\big(1-u_1(t)\big)\lambda S(t)\\-(1-\epsilon_1)\lambda V(t)\\\big(1-u_1(t)\big)\lambda S(t)+u_2(1-\epsilon_1)\lambda V(t)\\0\\0\\0\\0\end{pmatrix}. \tag{39}$$

A nonlinear coupled system with bounded coefficients is shown by Eq. (37). Let

$$\mathcal{H}=\mathcal{D}(\psi)\mathcal{W}+\mathcal{G}(\psi,\mathcal{W}). \tag{40}$$

Hence, from the first equation of Eq. (39)

$$\mathcal{G}(\psi,\mathcal{W}_1)-\mathcal{G}(\psi,\mathcal{W}_2)=\{-(1-u_1(t))\lambda S_1\}-\{-(1-u_1(t))\lambda S_2\}$$
$$|\mathcal{G}(\psi,\mathcal{W}_1)-\mathcal{G}(\psi,\mathcal{W}_2)|\le|-(1-u_1(t))(\lambda_1-\lambda_2)|.$$

thus,

$$|\mathcal{G}(\psi,\mathcal{W}_1)-\mathcal{G}(\psi,\mathcal{W}_2)|\le|1-u1(t)||\beta|(|\tau||E_1-E_2|+|\nu||C_1-C_2|+|I_1-I_2|). \tag{41}$$

This shows that $\mathcal{G}(\psi,\mathcal{W})$ satisfies a Lipschitz condition in $\mathcal{W}$, since the right-hand side is bounded by a product of bounded terms. Also,

$$\mathcal{D}(\psi)\mathcal{W}_1-\mathcal{D}(\psi)\mathcal{W}_2=\{-(\kappa+\mu)S_1+\omega V_1+0R_1\}-\{-(\kappa+\mu)S_2+\omega V_2+0R_2\}$$
$$|\mathcal{D}(\psi)\mathcal{W}_1-\mathcal{D}(\psi)\mathcal{W}_2|\le|(\kappa+\mu)||S_1-S_2|+|\omega||V_1-V_2|+|0||R_1-R_2| \tag{42}$$

Thus, Eq. (40) becomes

$$|\mathcal{H}(\mathcal{W}_1)-\mathcal{H}(\mathcal{W}_2)|\le C(|S_1-S_2|+|V_1-V_2|+|R_1-R_2|+|C_1-C_2|+|E_1-E_2|+|I_1-I_2|+|T_1-T_2|),$$

where $C=\max\{|C_1|,|C_2|,|C_3|,|C_4|,|C_5|,|C_6|,|C_7|\}$ is a positive constant independent of the state variables.

Furthermore,

$$|\mathcal{H}(\mathcal{W}_1)-\mathcal{H}(\mathcal{W}_2)|\le\mathcal{P}|\mathcal{W}_1-\mathcal{W}_2|,$$

where $\mathcal{P}=\sum_{i=1}^{7}J_i+|\mathcal{M}|<\infty$ is a finite positive constant.

This implies that $\mathcal{H}(\mathcal{W})$ is uniformly Lipschitz continuous. Therefore, a unique solution to the optimal control system exists.

3. The Lagrangian defined in Eq. (36) is convex with respect to the control variables.
Using Eq. (36), let

$$\mathcal{L}(x,u,t)=\mathcal{L}_1(x,t)+\mathcal{L}_2(u,t), \tag{43}$$

where

$$\mathcal{L}_1(x,t)=\kappa_1E+\kappa_2C+\kappa_3I, \tag{44}$$

$$\mathcal{L}_2(u,t)=\frac{1}{2}\sum_{i=1}^{3}\xi_iu_i^2(t). \tag{45}$$

The objective is to show that the term $\mathcal{L}_2(u,t)$ is convex. Define the function $\psi_i\colon[0,1]^3\to\mathbb{R}$ by $\psi_i(u,t)=\frac{1}{2}u_i^2(t)$, for $i=1,2,3$. Then, for any $q,v\in[0,1]^3$ and $\lambda\in[0,1]$:

$$\lambda\psi(q)+(1-\lambda)\psi(v)\ge\psi(\lambda q+(1-\lambda)v),$$

which satisfies the definition of convexity. Hence, $\mathcal{L}_2(u,t)$ is convex with respect to the control variable u.

4. There exist positive constants n_1,n_2 and $n_3>1$ such that the Lagrangian Eq. (36) is bounded below by an expression of the form

$$n_1\|u\|^{n_3/2}-n_2.$$

From Eq. (45), it follows that

$$\mathcal{L}(x,u,t) \geq \frac{1}{2}\sum_{i=1}^{3}\xi_i u_i^2(t) \geq n_1\left(\sum_{i=1}^{3} \| u_i(t) \|^2\right)^{\frac{n_3}{2}} - n_2, \tag{46}$$

where $n_1 = \frac{1}{2}\min(\xi_i)$, $n_2 > 0$, and $n_3 = 2$. This inequality provides a lower bound for the Lagrangian, ensuring it satisfies the convexity condition necessary for the existence of an optimal control. ■

To establish the optimal control characterization, the Hamiltonian function $\mathcal{H}$ associated with the OCP is defined as:

$$\begin{aligned}
\mathcal{H} \quad &= \mathcal{L}(x,u,t) + \textstyle\sum_{j=1}^{7} \lambda_j \cdot \dot{X}_j(t) \\
&= (\kappa_1 E + \kappa_2 C + \kappa_3 I() + \tfrac{1}{2}\big(\xi_1 u_1^2(t) + \xi_2 u_2^2(t) + \xi_3 u_3^2(t)\big) \\
&\quad +\lambda_S\big(\alpha + \omega V - \kappa S - \big(1-u_1(t)\big)\lambda S - \mu S\big) \\
&\quad +\lambda_V(\kappa S - u_2(1-\epsilon_1)\lambda V - \omega V - \mu V) \\
&\quad +\lambda_E\left(\big(1-u_1(t)\big)\lambda S + u_2(1-\epsilon_1)\lambda V - \sigma_1 E - \big(1-u_3(t)\big)\sigma_2 E - \sigma_3 E - \mu E\right) \\
&\quad +\lambda_C\big(\sigma_1 E - \big(1-u_3(t)\big)\gamma C - \mu C\big) \\
&\quad +\lambda_I\left(\big(1-u_3(t)\big)\sigma_2 E + \big(1-u_3(t)\big)\gamma\rho C - \eta_1 I - \delta I - \mu I\right) \\
&\quad +\lambda_T(\eta_1\epsilon_2 I - \eta_2 T - \delta T - \mu T) \\
&\quad +\lambda_R\big(\sigma_3 E + \big(1-u_3(t)\big)\gamma(1-\rho)C + \eta_1(1-\epsilon_2)I + \eta_2 T - \mu R\big),
\end{aligned} \tag{47}$$

where λ_j for $j = (S,V,E,C,I,T,R)$ represents the adjoint variables for the corresponding state variables.

Theorem 6. *Given the optimal control variables u_i for $i = 1,2,3$ and the solutions of the state variables $S^*, V^*, E^*, C^*, I^*, T^*, R^*$, there exist adjoint variables λ_j for $j = S,V,E,C,I,T,R$ satisfying:*

$$\dot{\lambda}_S = -\lambda_S(-\kappa - (1-u_1)\beta(\nu C + \tau E + I) - \mu) - \lambda_V\,\kappa - \lambda_E(1-u_1)\beta(\nu C + \tau E + I), \tag{48}$$

$$\dot{\lambda}_V = -\lambda_S\,\omega - \lambda_V(-u_2(1-\epsilon_1)\beta(\nu C + \tau E + I) - \omega - \mu) - \lambda_E\,u_2(1-\epsilon_1)\beta(\nu C + \tau E + I), \tag{49}$$

$$\begin{aligned}
\dot{\lambda}_E = &-\kappa_1 + \lambda_S(1-u_1)\beta\tau S + \lambda_V u_2(1-\epsilon_1)\beta\tau V \\
&-\lambda_E\big((1-u_1)\beta\tau S + u_2(1-\epsilon_1)\beta\tau V - \sigma_1 - (1-u_3)\sigma_2 - \sigma_3 - \mu\big) \\
&-\lambda_C\sigma_1 - \lambda_I(1-u_3)\sigma_2 - \lambda_R\sigma_3,
\end{aligned} \tag{50}$$

$$\begin{aligned}
\dot{\lambda}_C = &-\kappa_2 + \lambda_S(1-u_1)\beta\,\nu\,S + \lambda_V u_2(1-\epsilon_1)\beta\,\nu\,V - \lambda_E\big((1-u_1)\beta\,\nu\,S + u_2(1-\epsilon_1)\beta\,\nu\,V\big) \\
&-\lambda_C(-(1-u_3)\gamma - \mu) - \lambda_I(1-u_3)\gamma\,\rho - \lambda_R(1-u_3)\gamma(1-\rho),
\end{aligned} \tag{51}$$

$$\begin{aligned}
\dot{\lambda}_I = &-\kappa_3 + \lambda_S(1-u_1)\beta\,S + \lambda_V u_2(1-\epsilon_1)\beta\,V - \lambda_E\big((1-u_1)\beta\,S + u_2(1-\epsilon_1)\beta\,V\big) \\
&-\lambda_I(-\eta_1 - \delta - \mu) - \lambda_T\,\epsilon_2\,\eta_1 - \lambda_R\,\eta_1(1-\epsilon_2),
\end{aligned} \tag{52}$$

$$\dot{\lambda}_T = -\lambda_T(-\delta - \mu - \eta_2) - \lambda_R\,\eta_2, \tag{53}$$

$$\dot{\lambda}_R = \lambda_R\,\mu. \tag{54}$$

Given the transversality conditions:

$$\lambda_j(t_f) = 0, \quad \text{for} \quad j \in \{S,V,E,C,I,T,R\}, \tag{55}$$

and the characterization of the control variables given as:

$$u_1^*(t) = min\left\{1, max\left\{0, -\frac{(\lambda_S - \lambda_E)\beta\,(C\nu + E\tau + I)S}{\xi_1}\right\}\right\},$$

$$u_2^*(t) = min\left\{1, max\left\{0, \frac{(\lambda_V - \lambda_E)(1-\epsilon_1)\beta(\nu C + \tau E + I)V}{\xi_2}\right\}\right\},$$

$$u_3^*(t) = min\left\{1, max\left\{0, \frac{-\lambda_E\sigma_2 E - \lambda_C\gamma C - \lambda_I(-\gamma\rho C - \sigma_2 E) + \lambda_R\gamma(1-\rho)C}{\xi_3}\right\}\right\},$$

minimizes $J(u_1^*, u_2^*, u_3^*)$ over Φ.

Proof. If $(\mathbf{x}, \mathbf{u})$ denotes the optimal solution of the control problem, then $\frac{\partial \mathcal{H}}{\partial \mathbf{u_1}} = \frac{\partial \mathcal{H}}{\partial \mathbf{u_2}} = \frac{\partial \mathcal{H}}{\partial \mathbf{u_3}} = \mathbf{0}$ at $\mathbf{u_i} = \mathbf{u_i^*}$.

Hence,

$$\frac{\partial \mathcal{H}}{\partial u_1} = -\xi_1 u_1 - \lambda_S \beta\,(Cv + E\tau + I)S + \lambda_E \beta\,(Cv + E\tau + I)S,$$
$$\frac{\partial \mathcal{H}}{\partial u_2} = -\xi_2 u_2 + \lambda_V (1-\epsilon_1)\beta\,(Cv + E\tau + I)V - \lambda_E (1-\epsilon_1)\beta\,(Cv + E\tau + I)V,$$
$$\frac{\partial \mathcal{H}}{\partial u_3} = -\xi_3 u_3 - \lambda_E \sigma_2 E - \lambda_C \gamma\, C - \lambda_I(-C\gamma\,\rho - E\sigma_2) + \lambda_R \gamma\,(1-\rho)C.$$

Consequently, the optimal control functions are expressed as

$$\begin{cases} u_1^* = -\dfrac{(\lambda_S - \lambda_E)\beta\,(Cv + E\tau + I)S}{\xi_1} \\ u_2^* = \dfrac{(\lambda_V - \lambda_E)(1-\epsilon_1)\beta(vC + \tau E + I)V}{\xi_2} \\ u_3^* = \dfrac{-\lambda_E \sigma_2 E - \lambda_C \gamma C - \lambda_I(-\gamma\rho C - \sigma_2 E) + \lambda_R \gamma(1-\rho)C}{\xi_3} \end{cases} \tag{56}$$

Finally, according to the standard definition of control, and by applying the bounds on u_i^*,

$$u_i^* = \begin{cases} 0 \;\; if \;\; \vartheta_i^* \le 0 \\ \vartheta_i^* \;\; if \;\; 0 < \vartheta_i^* < 1 \\ 1 \;\; if \;\; \vartheta_i^* \ge 0 \end{cases} \text{ for } i = 1,2,3 \text{ and}$$

$$\vartheta_1 = -\frac{(\lambda_S - \lambda_E)\,\beta\,(Cv + E\tau + I)\,S}{\xi_1}$$

$$\vartheta_2 = \frac{(\lambda_V - \lambda_E)(1-\epsilon_1)\beta(vC + \tau E + I)V}{\xi_2}$$

$$\vartheta_3 = \frac{-\lambda_E \sigma_2 E - \lambda_C \gamma C - \lambda_I(-\gamma\rho C - \sigma_2 E) + \lambda_R \gamma(1-\rho)C}{\xi_3}$$

Hence, each of the control measures is written in compact form as follows:

$u_1^* = min\{1, max\{0, \vartheta_1\}\},\; u_2^* = min\{1, max\{0, \vartheta_2\}\}$, and $u_3^* = min\{1, max\{0, \vartheta_3\}\}$. ■

3.5 Numerical Solutions

In this section, the numerical simulation of the proposed meningitis model is carried out. The numerical solution to the model in Eq. (1) is computed using the MATLAB ODE45 solver, which is well-suited for handling non-stiff ordinary differential equation systems, subject to the following initial conditions (in millions):

$$S(0) = 8.7,\quad V(0) = 4.5,\quad E(0) = 4.2,\quad C(0) = 3.5,\quad I(0) = 3.1,\quad T(0) = 2.5,\quad R(0) = 1.6.$$

The parameter values used, which are mostly obtained from published literature, are presented in Table 1. Graphs of the population dynamics against time, ranging from 0 to 50 days, are plotted for the model in Eq. (1). Employing the parameter values listed in Table 1, $\mathbb{R}_0$ for system in Eq. (1) is calculated to be approximately $\mathbb{R}_0 = 1.623$, highlighting the need for optimal control interventions. In order to evaluate the efficiency of control strategies, the interventions are divided into three distinct strategies, and their impacts on the model dynamics are analyzed. According to the World Health Organization release, Prophylactic chemoprophylaxis is a frontline defense in meningitis control, particularly for preventing secondary transmission, containing outbreaks, and protecting high-risk contacts, complementing vaccination efforts [16] and thus, is a key element for preventing the disease. As a result, each of the three control strategies in this study included this preventive intervention.

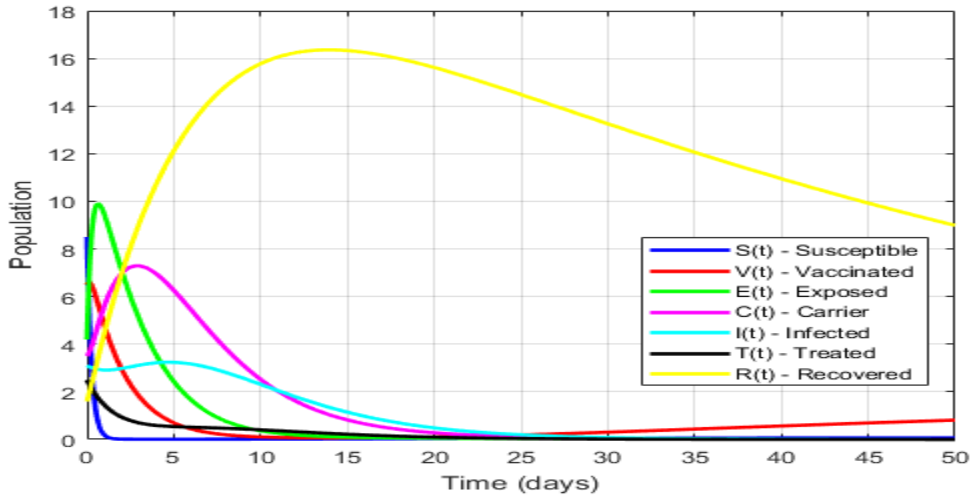

Figure 2. Population Dynamics of Meningitis for each Compartment Throughout a 50-Day Span

Fig. 2 shows the population dynamics of the meningitis disease over a period of 0–50 days. From the graph, the susceptible population $S(t)$ decreases rapidly within the first few days and thereafter remains relatively stable because of the progression rate and the effect of vaccination. Because no other control measure has been implemented at this stage, the availability of vaccines for meningitis treatment, and the vaccinated population $V(t)$ increases sharply from day 30 onward, as shown in the graph. The rapid decrease of the vaccination population within the first few days is a result of the progression rate, including the vaccine waning rate, leading to the exposed compartment. The exposed individuals $E(t)$ initially increase, reflecting the progression from both the susceptible and vaccinated classes, and subsequently decline due to successful detection, treatment, and immunity development. The carrier population $C(t)$ increases steadily within the first few days and then decreases due to the progression of carriers into the infected class between days 5 and 20. It remains relatively stable from day 21 onward, indicating good compliance with vaccination efforts or an increase in vaccine intake.

Furthermore, the infected population $I(t)$ shows a slight increase in the number of infected individuals within days 0–10, and thereafter decreases. The treated population $T(t)$ decreases rapidly within the first 0–5 days, contributing to the significant rise in the recovered population $R(t)$ within days 0–15. This is followed by a decline due to the decrease in the number of infected and treated individuals.

Strategy 1: A combination of optimal control, public health education, and prophylactic chemoprophylaxis administration (i.e., $u_1(t) \neq 0, u_2(t) = 0$, and $u_3(t) \neq 0$)

This strategy combines public health education campaigns with prophylactic chemoprophylaxis administration against meningitis. The simulation results in Fig. 3 (a)–Fig. 3 (e) show a clear reduction in disease transmission compared to the no-control case. Fig. 3 (a) reveals that the number of exposed individuals drops sharply under control, while remaining high without intervention. In Fig. 3 (b), carrier numbers initially rise slightly within the first few days, then fall rapidly under control, in contrast to the sustained peak observed without control. Similarly, Fig. 3 (c) shows that infected individuals decrease significantly under control, highlighting the effectiveness of early interventions. Fig. 3 (d) indicates that fewer individuals require treatment in the early days due to reduced infections. After day 30, the treated population under control becomes slightly higher than in the uncontrolled case, reflecting targeted case management. As shown in Fig. 3 (e), the number of recovered individuals increases sharply under control, driven by public health education and chemoprophylaxis, before gradually declining as new infections diminish. Finally, Fig. 3 (f) presents the control profiles over time. Public health education is applied strongly in the early phase, while chemoprophylaxis is maintained at key intervals to suppress transmission. In general, this combined approach significantly reduces both the spread and persistence of meningitis.

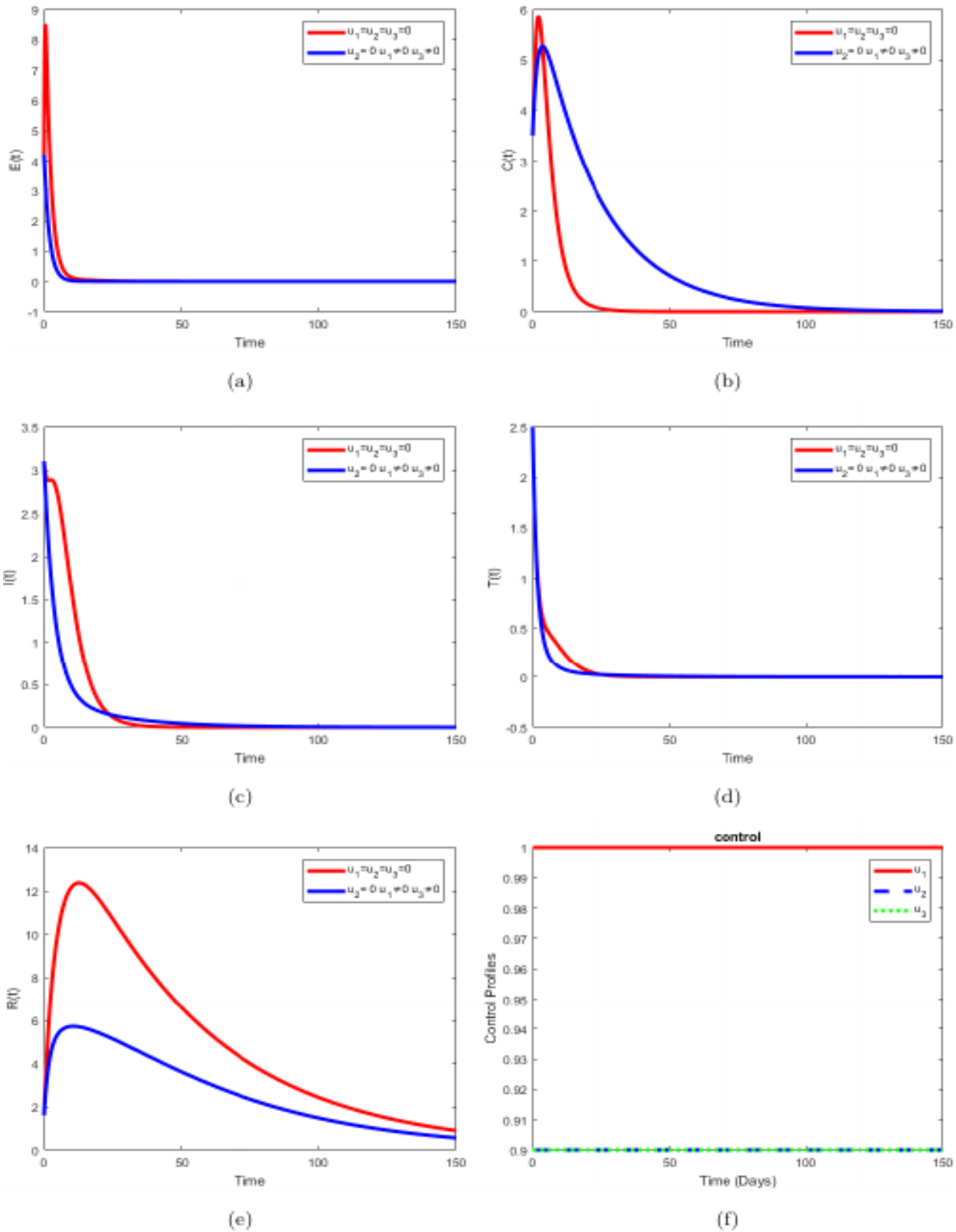

Figure 3. Effects of Optimal Use of Strategy 1 on the Population Dynamics of Meningitis (a) Exposed Humans (b) Carrier Humans (c) Infected Humans (d) Treated Humans (e) Recovered Humans (f) Control Profiles

Strategy 2: A combination of booster vaccine administration and prophylactic chemoprophylaxis administration (i.e., $u_1(t) = 0$, $u_2(t) \neq 0$, and $u_3(t) \neq 0$)

This strategy combines booster vaccine administration with prophylactic chemoprophylaxis. The simulation results in Fig. 4 (a)–Fig. 4 (e) reveal a marked reduction in transmission compared to the no-control case. Fig. 4 (a) shows that the number of exposed individuals drops sharply under control. In Fig. 4 (b), carriers increase rapidly in the first few days before declining due to the combined effects of vaccination and chemoprophylaxis. As seen in Fig. 4 (c), infected individuals decrease significantly within the first 70 days in

the controlled scenario, compared to sustained higher levels without intervention. This decline corresponds to Fig. 4 (d), where the treated population initially falls sharply in the first 20 days, then experiences a slight rise from day 30 onward. Fig. 4 (e) shows that recovered individuals increase rapidly during the first few days, then begin to decline under control, reflecting reduced infection levels. Finally, Fig. 4 (f) presents the control profiles over time, indicating that both booster vaccination and chemoprophylaxis are applied most intensively in the early phase, then adjusted as disease transmission subsides. Overall, this strategy demonstrates that combining vaccination with preventive drug administration effectively suppresses meningitis spread and accelerates recovery.

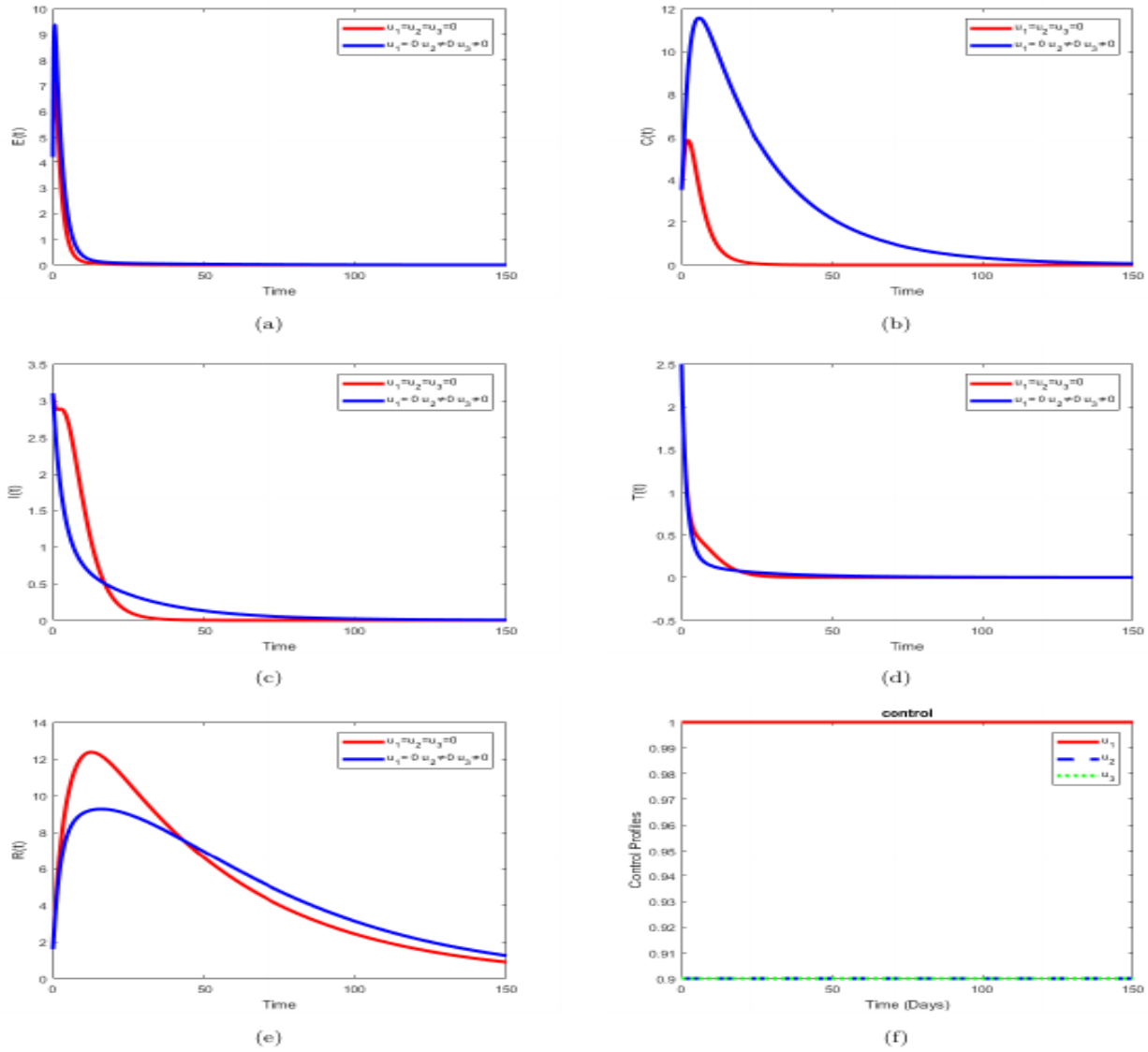

Figure 4. Effects of Optimal Use of Strategy 2 on the Population Dynamics of Meningitis (A) Exposed Humans (B) Carrier Humans (C) Infected Humans (D) Treated Humans (E) Recovered Humans (F) Control Profiles

Strategy 3: A combination of optimal public health education campaigns, booster vaccine administration, and prophylactic chemoprophylaxis administration (i.e $u_1(t) \neq 0$, $u_2(t) \neq 0$, and $u_3(t) \neq 0$)

In this strategy, all the introduced control measures, public health education campaigns, booster vaccine administration, and prophylactic chemoprophylaxis administration are implemented against meningitis. The simulation results in Fig. 5 (a)–Fig. 5 (e) show that this integrated approach produces the most significant reduction in disease burden. Fig. 5 (a) reveals an initial rise in exposed individuals during the first few days, followed by a sharp decline between days under control, in contrast to the sustained high levels without intervention. In Fig. 5 (b), carrier numbers increase rapidly, then drop steeply from day 25 as the combined measures take effect. Fig. 5 (c) shows a marked reduction in infected individuals under control, before converging with the uncontrolled case from day 70 onward. As shown in Fig. 5 (d), the number of treated individuals remains lower under control due to reduced infections. Fig. 5 (e) presents a steep rise in recovered

individuals during the first 25 days, followed by a gradual decline, reflecting the sustained suppression of transmission through the combined strategies. Finally, Fig. 5 (f) illustrates the timing and intensity of each intervention, showing strong early application of all three measures with adjustments over time. Overall, this integrated strategy proves highly effective in reducing transmission, limiting illness, and promoting faster recovery.

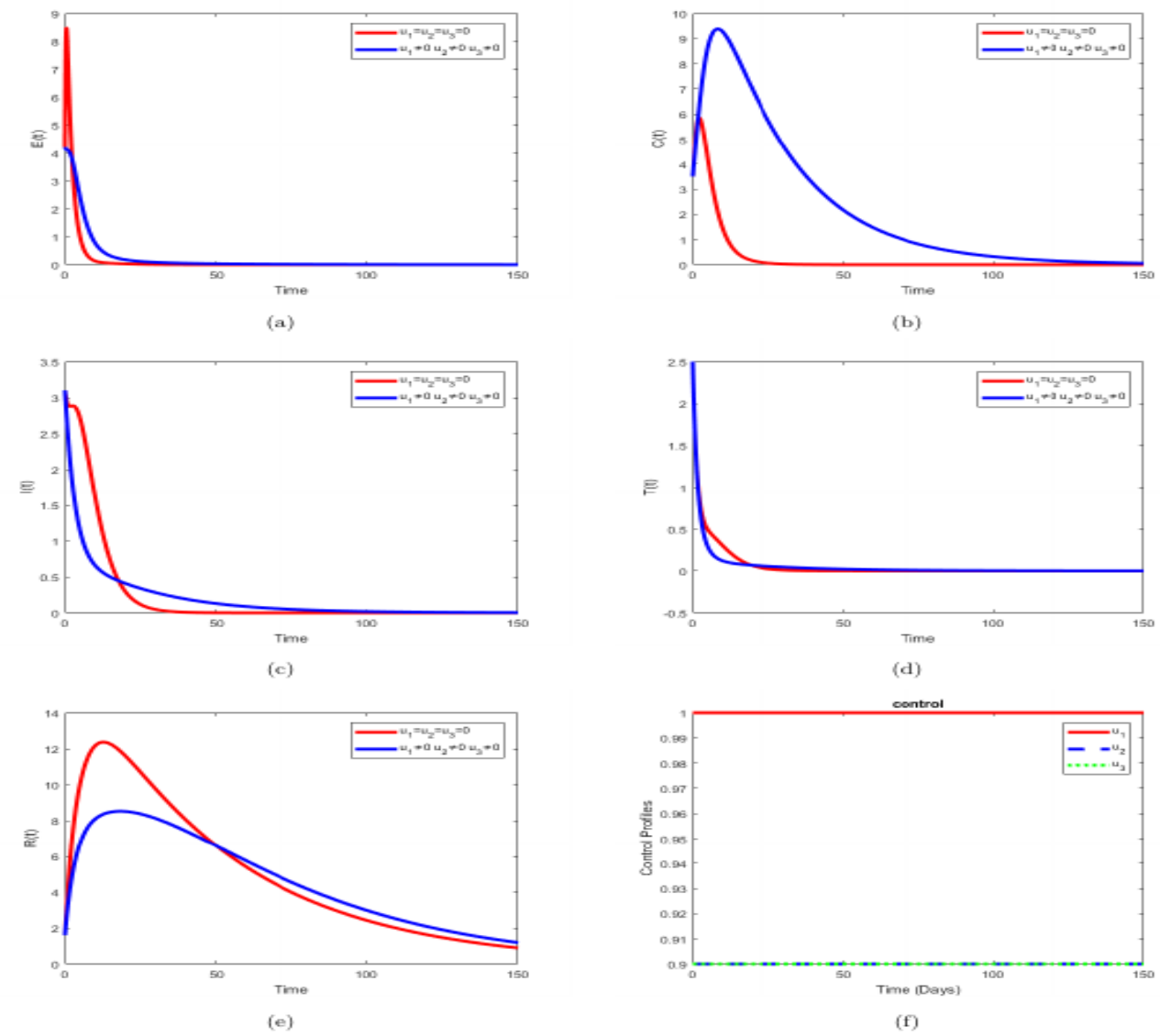

Figure 5. Effects of Optimal Use of Strategy 3 on the Population Dynamics of Meningitis (a) Exposed Humans (b) Carrier Humans (c) Infected Humans (d) Treated Humans (e) Recovered Humans (f) Control Profiles

3.6 Cost-Effectiveness Analysis

To evaluate the economic efficiency of the proposed intervention strategies in mitigating the spread of meningitis, a cost-effectiveness analysis is carried out. This approach helps determine whether the health benefits derived from the controls justify the associated costs [8], [50], [51]. In particular, key performance metrics such as the IAR, ACER, and ICER are carried. The IAR measures the proportion of infections prevented through intervention, while ACER and ICER provide insights into the cost per infection averted, facilitating comparison across control strategies. These metrics collectively guide the identification of the most cost-effective approach for controlling meningitis transmission [50], [55].

3.6.1 Infection Averted Ratio (IAR)

The number of infections avoided by implementing a control plan is measured by the IAR, which is defined as follows:

$$\text{IAR} = \frac{\text{Cumulative cases averted}}{\text{Total number of recovered individuals}}.$$

The number of infections averted is calculated by subtracting the total number of infectious individuals under the control strategy from those recorded without any intervention. A higher IAR value reflects greater effectiveness of the strategy in reducing infections [52], [56]. Therefore, the most cost-effective control method is the one that produces the highest IAR. Each strategy's IAR is assessed using the parameter values in Table 1. Fig. 6 (a) presents the IAR values with and without control for each proposed strategy.

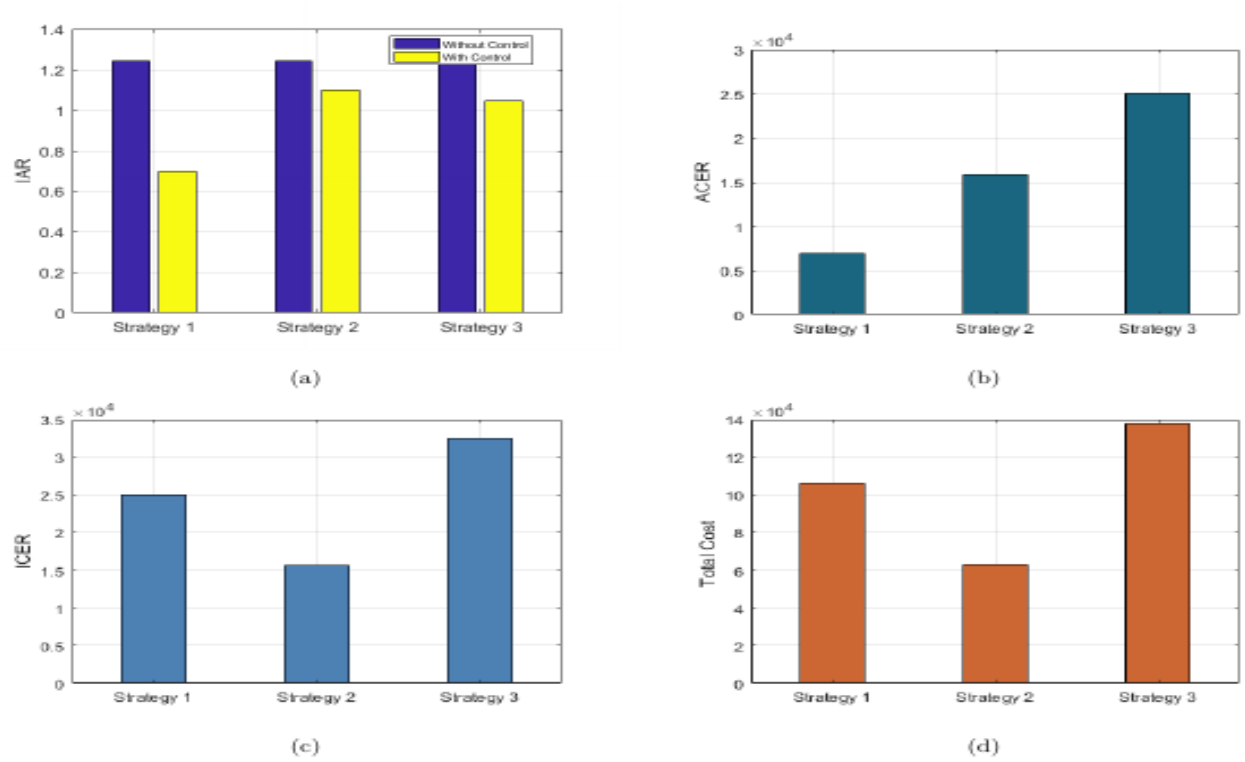

Figure 6. Cost-effectiveness Analysis (a) IAR, (b) ACER, (c) ICER, and (d) Total Cost

Based on the results in Fig. 6 (a), Strategy 2 yields the highest IAR value of 1.0995. Therefore, Strategy 2 is considered the most cost-effective among the three. This is followed by Strategy 3 with an IAR of 1.0453, indicating the second most cost-effective approach. Strategy 1, which combines public health education and chemoprophylaxis, has the lowest IAR of 0.6980 and is thus considered the least cost-effective. This suggests that combining education campaigns alone with chemoprophylaxis, without booster vaccination, may not significantly reduce the infection burden.

3.6.2 Average Cost-Effectiveness Ratio (ACER)

The ACER provides a quantitative measure of the economic efficiency of a given intervention strategy. Specifically, it represents the cost required to avert a single case of infection through that strategy [18], [32], [57], [58]. Mathematically, ACER is defined as:

$$\text{ACER} = \frac{\text{Total cost of implementing the strategy}}{\text{Cumulative number of infections averted}}.$$

The total cost associated with a control strategy is computed using the objective functional defined in Eq. (33), which aggregates both the health costs and the costs of applying the controls over the intervention period. A lower ACER value indicates a more economically favorable intervention. The computed ACER values for each strategy are summarized in Table 4.

Table 4. Cost-Effectiveness Analysis Values

Strategy	Cumulative Cases Averted	TC with control	ACER	ICER
Strategy 1	15.26	106234.2970	6959.40	25026.3
Strategy 2	3.98	62931.9548	15803.40	15635.0
Strategy 3	15.26	137753.4030	25025.58	32459.8

Based on the ACER results, Strategy 1 has the lowest ACER value of 6959.4016. This implies it is the most cost-effective strategy in terms of cost per infection averted. It is followed by Strategy 2 with an ACER of 15803.3896. Strategy 3, which combines all three controls, yields the highest ACER value (25025.5816), indicating that although it may avert more infections, it is less efficient economically. Therefore, based on ACER analysis, Strategy 1 is the most cost-effective approach (See Fig. 6 (b)).

3.6.3 Incremental Cost-Effectiveness Ratio (ICER)

The ICER is a key metric used to evaluate the additional cost incurred per infection averted when a control strategy is implemented compared to no intervention [5], [15], [38], [59]. It is expressed as:

$$\text{ICER} = \frac{C_{\text{control}} - C_{\text{nocontrol}}}{I_{\text{nocontrol}} - I_{\text{control}}},$$

where:

C_{control} is the total cost with control;
$C_{\text{nocontrol}}$ is the total cost without control;
$I_{\text{nocontrol}}$ is the total number of infections without control;
I_{control} is the total number of infections with control.

Using this formula and the approach in [60], the ICER values for the three control strategies are presented in Table 4 and Fig. 6 (c) below:

Among the strategies, Strategy 2 yields the lowest ICER, indicating it is the most cost-effective in reducing the number of infections. Strategy 3 has the highest ICER, making it the least cost-effective, while Strategy 1 lies in between. This analysis supports prioritizing booster vaccination and prophylactic chemoprophylaxis administration when resources are limited.

4. CONCLUSION

This study employs a mathematical model of meningitis transmission, extended into an optimal control framework, to evaluate the impact of combined interventions**.** The results demonstrate that targeted combinations of interventions can substantially suppress meningitis transmission, with notable implications for public health policy in endemic regions. Extending the model into an optimal control framework, three time-dependent controls: public health education campaigns (u_1), booster vaccine administration (u_2), and prophylactic chemoprophylaxis (u_3) are introduced. Analytical results and numerical simulations obtained via Pontryagin's Maximum Principle and solved using MATLAB revealed that all three tested strategies, each combining at least two controls, reduced the number of exposed, carrier, and infectious individuals. Using the ACER and ICER, the cost-effectiveness study revealed that Strategy 2 (booster vaccination and prophylactic chemoprophylaxis) delivered the greatest economic advantage, achieving the lowest cost per infection averted and the most favorable incremental benefit, making it the optimal choice in resource-limited settings. Although other strategies also reduced transmission, the combined vaccination and chemoprophylaxis approach consistently outperformed alternatives in both epidemiological and economic terms. Based on these findings, it is recommend that public health authorities in meningitis endemic regions should prioritize and sustained booster vaccination and chemoprophylaxis programs, integrate these pharmaceutical measures with targeted public health education campaigns to enhance community awareness and compliance and maintain robust surveillance systems to adjust intervention intensity as disease dynamics evolve, thereby ensuring efficient resource utilization and moving closer to the long-term elimination of the disease. A key limitation of this study is that the model relies on assumptions such as homogeneous mixing, constant parameter values, and idealized intervention efficacy, which may not fully capture real-world heterogeneities and stochastic effects in meningitis transmission. Future work should incorporate spatial dynamics, seasonality, and population heterogeneity to improve the predictive accuracy and applicability of the model.

Author Contributions

Ayodeji Sunday Afolabi: Conceptualization, Data Curation, Formal Analysis, Investigation, Methodology, Project Administration, Resources, Software, Supervision, Validation, Visualization, Writing–Original Draft, Review and Editing. Abdulwahab Ridwan: Data Curation, Formal Analysis, Investigation, Methodology, Project Administration, Resources, Software, Supervision, Validation, Visualization, Writing - Original Draft,

Writing- Review and Editing. Princess Chiamaka Uche: Data Curation, Formal Analysis, Investigation, Methodology, Project Administration, Resources, Software, Supervision, Validation, Visualization, Writing - Original Draft, Review and Editing. All authors discussed the results and contributed to the final manuscript.

Funding Statement

This research received no specific grant from any funding agency in the public, commercial, or not-for-profit sectors.

Acknowledgment

The authors sincerely appreciate the valuable comments and constructive suggestions provided by the reviewers.

Declarations

The authors declare no competing interests.

Declaration of Generative AI and AI-assisted Technologies

Generative AI tools (e.g., ChatGPT) were used solely for language refinement, including grammar, spelling, and clarity. The scientific content, analysis, interpretation, and conclusions were developed entirely by the authors. All final text was reviewed and approved by the authors.

REFERENCES

[1] M. V. Crankson, O. Olotu, and A. S. Afolabi, "MODELLING THE VACCINATION CONTROL OF BACTERIAL MENINGITIS TRANSMISSION DYNAMICS: A CASE STUDY," *Mathematical Modelling and Control*, vol. 3, no. 4, p. 416–434, 2023. doi: https://doi.org/10.3934/mmc.2023033

[2] N. K-D. O. Opoku, *et al*., "MODELLING THE TRANSMISSION DYNAMICS OF MENINGITIS AMONG HIGH AND LOW-RISK PEOPLE IN GHANA WITH COST-EFFECTIVENESS ANALYSIS," in *Abstract and Applied Analysis*, 2022. doi: https://doi.org/10.1155/2022/9084283

[3] World Health Organization, "DEFEATING MENINGITIS BY 2030: A GLOBAL ROADMAP," WHO Technical Report, World Health Organization, Geneva, 2025.

[4] N. A. F. A. Hamid, T. K. Ang, and F. M. Siam, *MODELLING OF THE SPREAD OF MENINGITIS DISEASE USING SEIR MODEL*.

[5] M. A. Belay, J. A. Okelo, D. M. Theuri, "MATHEMATICAL MODEL ANALYSIS FOR THE TRANSMISSION DYNAMICS OF BACTERIAL MENINGITIS DISEASE INCORPORATING DRUG-RESISTANCE CLASS," *Commun. Math. Biol. Neurosci*., vol. 2022, p. Article–ID, 2022.

[6] M. V. Crackson, O. Olotu, A. S. Afolabi, and A. Abidemi, "MATHEMATICAL MODELING AND STABILITY ANALYSES ON THE TRANSMISSION DYNAMICS OF BACTERIAL MENINGITIS," *J. Math. Comput. Sci*., vol. 11, no. 6, p. 7384–7413, 2021.

[7] Y. H. Workineh and S. M. Kassa, "OPTIMAL CONTROL OF THE SPREAD OF MENINGITIS: IN THE PRESENCE OF BEHAVIOUR CHANGE OF THE SOCIETY AND INFORMATION DEPENDENT VACCINATION," *Commun. Math. Biol. Neurosci*., vol. 2021, p. Article–ID, 2021.

[8] H. Christensen, C. L. Trotter, M. Hickman, and W. J. Edmunds, "EPIDEMIOLOGICAL IMPACT AND COST-EFFECTIVENESS OF UNIVERSAL VACCINATION WITH BEXSERO® TO REDUCE MENINGOCOCCAL GROUP B DISEASE IN GERMANY," *Vaccine*, vol. 34, no. 29, p. 3412–3419, 2016. doi: https://doi.org/10.1016/j.vaccine.2016.04.004

[9] K. G. Varshney and Y. K. Dwivedi. "MATHEMATICAL MODELLING OF INFLUENZA-MENINGITIS UNDER THE QUARANTINE EFFECT OF INFLUENZA," *Turkish Journal of Computer and Mathematics Education*, vol. 12, no. 11, pp. 7214-7225, 2021.

[10] C. Ngari, J. S. Kilonzi, C. G. Ngari, and M. K. James, *A NOVEL MODEL FOR TRANSMISSION DYNAMICS OF BACTERIAL MENINGITIS INCORPORATING VACCINATION AND TREATMENT USING COUNTERFEIT AND NON-COUNTERFEIT DRUGS*, SSRN 4951636.

[11] K. K. Danquah, S. T. Appiah, B. A. Danquah, B. A. Afful, and G. A. Safo, "GLOBAL ANALYSIS OF MENINGITIS DISEASE WITH OPTIMAL CONTROL," *Global analysis of meningitis disease with optimal control*, vol. 4, pp. 21-21, 2024. doi: https://doi.org/10.28924/ada/ma.4.21

[12] J. K. K. Asamoah, F. Nyabadza, B. Seidu, M. Chand, and H. Dutta, "MATHEMATICAL MODELLING OF BACTERIAL MENINGITIS TRANSMISSION DYNAMICS WITH CONTROL MEASURES," *Computational and Mathematical Methods in Medicine*, vol. 2018, no. 1, p. 2657461, 2018. doi: https://doi.org/10.1155/2018/2657461

[13] M. A. Belay, J. A. Okelo, D. M. Theuri, H. T. Alemneh, and N. Y. Alemu, "A COINFECTION MODEL OF BACTERIAL MENINGITIS AND HEPATITIS B DISEASES WITH OPTIMAL CONTROL AND COST-EFFECTIVENESS ANALYSIS," *Journal of Applied Mathematics*, vol. 2025, no. 1, p. 9015761, 2025. doi: https://doi.org/10.1155/jama/9015761

[14] D. V. de Beek, M. C. Brouwer, G. E. Thwaites, and A. R. Tunkel, "ADVANCES IN TREATMENT OF BACTERIAL MENINGITIS," *The Lancet*, vol. 380, no. 9854, p. 1693–1702, 2012. doi : https://doi.org/10.1016/S0140-6736(12)61186-6

[15] P. S. Moore, "MENINGOCOCCAL MENINGITIS IN SUB-SAHARAN AFRICA: A MODEL FOR THE EPIDEMIC PROCESS," *Clinical Infectious Diseases*, vol. 14, no. 2, p. 515–525, 1992. doi: https://doi.org/10.1093/clinids/14.2.515

[16] W.H. Organization, "MENINGITIS," 2025. [Online]. Available: http://www.who.int/health-topics/meningitis. [Accessed 15 may 2025].

[17] M. A. Afolabi, K. S. Adewoye, A. I. Folorunso, and M. A. Omoloye, "A mathematical model on transmission dynamics of meningococcal meningitis," Iconic Research and Engineering Journal, vol. 4, pp. 59–66, 2021

[18] B. S. Kotola and T. T. Mekonnen, "MATHEMATICAL MODEL ANALYSIS AND NUMERICAL SIMULATION FOR CODYNAMICS OF MENINGITIS AND PNEUMONIA INFECTION WITH INTERVENTION," *Scientific Reports*, vol. 12, no. 1, p. 2639, 2022. doi: https://doi.org/10.1038/s41598-022-06253-0

[19] S. Tartof, *et al*., "IDENTIFYING OPTIMAL VACCINATION STRATEGIES FOR SEROGROUP A NEISSERIA MENINGITIDIS CONJUGATE VACCINE IN THE AFRICAN MENINGITIS BELT (VOL 8, E63605, 2013)," *PLOS ONE*, vol. 12, no. 12, 2017. doi: https://doi.org/10.1371/journal.pone.0190188

[20] A. Karachaliou, A. J. K. Conlan, M-P. Preziosi, and C. L. Trotter, "MODELING LONG-TERM VACCINATION STRATEGIES WITH MENAFRIVAC IN THE AFRICAN MENINGITIS BELT," *Clinical Infectious Diseases*, vol. 61, no. suppl 5, p. S594–S600, 2015. doi: https://doi.org/10.1093/cid/civ508

[21] I. A. Baba, L. I. Olamilekan, A. Yusuf, and D. Baleanu, *ANALYSIS OF MENINGITIS MODEL: A case study of northern Nigeria*, 2020.

[22] A. K. Prasinou, *USING MATHEMATICAL MODELS TO EVALUATE AND INFORM IMMUNISATION STRATEGIES WITH MENAFRIVAC IN THE AFRICAN MENINGITIS BELT, PhD thesis*, 2020.

[23] M. Y. Li, *AN INTRODUCTION TO MATHEMATICAL MODELING OF INFECTIOUS DISEASES*, *vol. 2*, Springer, 2018.

[24] P. A. W. J. Van den Driessche, "REPRODUCTION NUMBERS AND SUB-THRESHOLD ENDEMIC EQUILIBRIA FOR COMPARTMENTAL MODELS OF DISEASE TRANSMISSION," *Mathematical Biosciences*, vol. 180, no. 1-2, pp. 29-48, 2002. doi: https://doi.org/10.1016/S0025-5564(02)00108-6

[25] E. Vynnycky and R. White, *AN INTRODUCTION TO INFECTIOUS DISEASE MODELLING*, Oxford University Press, 2010.

[26] F. B. Agusto and M. C. A. Leite, "OPTIMAL CONTROL AND COST-EFFECTIVE ANALYSIS OF THE 2017 MENINGITIS OUTBREAK IN NIGERIA," *Infectious Disease Modelling*, vol. 4, 2019. doi: https://doi.org/10.1016/j.idm.2019.05.003

[27] J. K. K. Asamoah, F. Nyabadza, B. Seidu, M. Chand, and H. Dutta, "MATHEMATICAL MODELLING OF BACTERIAL MENINGITIS TRANSMISSION DYNAMICS WITH CONTROL MEASURES," *Computational and Mathematical Methods in Medicine*, vol. 2018, no. 1, p. 2657461, 2018. doi: https://doi.org/10.1155/2018/2657461

[28] J. A. Berkley, I. Mwangi, F. Mellington, S. Mwarumba, and K. Marsh, "CEREBRAL MALARIA VERSUS BACTERIAL MENINGITIS IN CHILDREN WITH IMPAIRED CONSCIOUSNESS," *QJM*, vol. 92, no. 3, p. 151–157, 1999. doi: https://doi.org/10.1093/qjmed/92.3.151

[29] T. Koutangni, *et al*., " COMPARTMENTAL MODELS FOR SEASONAL HYPERENDEMIC BACTERIAL MENINGITIS IN THE AFRICAN MENINGITIS BELT," *Epidemiology & Infection*, vol. 147, p. e14, 2019. doi: https://doi.org/10.1017/S0950268818002625

[30] M.J. F. Mart´ınez, E. G. Merino, E. G. S´anchez, J. E. G. S´anchez, A. M. Rey, and G. R. S´anchez. "A MATHEMATICAL MODEL TO STUDY THE MENINGOCOCCAL MENINGITIS," *Procedia Computer Science*, vol. 18, p. 2492–2495, 2013. doi: https://doi.org/10.1016/j.procs.2013.05.426

[31] K. Maseno, "MATHEMATICAL MODEL FOR MALARIA AND MENINGITIS CO-INFECTION AMONG CHILDREN," *Applied Mathematical Sciences*, vol. 5, no. 47, p. 2337–2359, 2011.

[32] K. B. Blyuss, "MATHEMATICAL MODELLING OF THE DYNAMICS OF MENINGOCOCCAL MENINGITIS IN AFRICA," in *UK Success Stories in Industrial Mathematics*, 2016, pp. 221-226. doi: https://doi.org/10.1007/978-3-319-25454-8_28

[33] H. Christensen, M. Hickman, W. J. Edmunds, and C. L. Trotter. "INTRODUCING VACCINATION AGAINST SEROGROUP B MENINGOCOCCAL DISEASE: AN ECONOMIC AND MATHEMATICAL MODELLING STUDY OF POTENTIAL IMPACT," *Vaccine*, vol. 31, no. 23, p. 2638–2646, 2013. doi: https://doi.org/10.1016/j.vaccine.2013.03.034

[34] H. Christensen, C. L. Trotter, M. Hickman, and W. J. Edmunds. "RE-EVALUATING COST EFFECTIVENESS OF UNIVERSAL MENINGITIS VACCINATION (BEXSERO) IN ENGLAND: MODELLING STUDY," *BMU*, vol. 349, 2014. doi: https://doi.org/10.1136/bmj.g5725

[35] K. du Preez, *et al*., "GLOBAL BURDEN OF TUBERCULOUS MENINGITIS IN CHILDREN AGED 0–14 YEARS IN 2019: A MATHEMATICAL MODELLING STUDY," *The Lancet Global Health*, vol. 13, no. 1, p. e59–e68, 2025. doi: https://doi.org/10.1016/S2214-109X(24)00383-8

[36] S. P. Gatyeni, "MATHEMATICAL MODELLING OF MENINGITIS TRANSMISSION DYNAMICS AND THE IMPACT OF VACCINATION STRATEGIES," SSRN 5291343, 2025. doi: https://doi.org/10.2139/ssrn.5291343

[37] S. S. Musa, S. Zhao, N. Hussaini, A. G. Habib, and D. He, "MATHEMATICAL MODELING AND ANALYSIS OF MENINGOCOCCAL MENINGITIS TRANSMISSION DYNAMICS," *International Journal of Biomathematics*, vol. 13, no. 01, p. 2050006, 2020. doi: https://doi.org/10.1142/S1793524520500060

[38] G. T. Tilahun, "OPTIMAL CONTROL ANALYSIS OF PNEUMONIA AND MENINGITIS COINFECTION," *Computational and Mathematical Methods in Medicine*, vol. 2019, no. 1, p. 2658971, 2019. doi: https://doi.org/10.1155/2019/2658971

[39] T. K. Yano, J. Bitok, and R. Jerop, "OPTIMAL CONTROL ANALYSIS OF MENINGOCOCCAL MENINGITIS DISEASE WITH VARYING POPULATION SIZE," *Applied and Computational Mathematics*, vol. 11.

[40] P. S. Moore, "MENINGOCOCCAL MENINGITIS IN SUB-SAHARAN AFRICA: A MODEL FOR THE EPIDEMIC PROCESS," *Clinical Infectious Diseases*, vol. 14, no. 2, p. 515–525, 1992. doi: https://doi.org/10.1093/clinids/14.2.515

[41] M. M. Ojo and E. F. D. Goufo. "MATHEMATICAL ANALYSIS OF A LASSA FEVER MODEL IN NIGERIA: OPTIMAL CONTROL AND COST-EFFICACY," *International Journal and Dynamics Control*, vol. 10, no. 6, p. 1807–1828, 2022. doi: https://doi.org/10.1007/s40435-022-00951-3

[42] S. Saber, A. M. Alghamdi, G. A. Ahmed, and K. M. Alshehri, "MATHEMATICAL MODELLING AND OPTIMAL CONTROL OF PNEUMONIA DISEASE IN SHEEP AND GOATS IN AL-BAHA REGION WITH COST-EFFECTIVE STRATEGIES," *AIMS Mathematics*, vol. 7, no. 7, pp. 12011-12049, 2022. doi: https://doi.org/10.3934/math.2022669

[43] A. Elsonbaty, T. M. Al-shami, and A. El-Mesady, "UNVEILING THE DYNAMICS OF MENINGITIS INFECTIONS: A COMPREHENSIVE STUDY OF A NOVEL FRACTIONAL-ORDER MODEL WITH OPTIMAL CONTROL STRATEGIES," *Boundary Value Problems*, vol. 2025, no. 1, p. 48, 2025. doi: https://doi.org/10.1186/s13661-025-02034-6

[44] S. T. Sulma and M. I. A. Kasbawati, "OPTIMAL CONTROL OF TRANSMISSION DYNAMICS OF MENINGITIS DISEASE WITH VACCINATION, CAMPAIGN, AND TREATMENT FACTORS".

[45] U. T. Mustapha, A.I. Muhammad, A. Yusuf, N. Althobaiti, A. I. Aliyu, and J. Andrawus, "MATHEMATICAL DYNAMICS OF MENINGOCOCCAL MENINGITIS: EXAMINING CARRIER DIAGNOSIS AND PROPHYLAXIS TREATMENT," *International Journal of Applied and Computational Mathematics*, vol. 11, no. 2, pp. 1-29, 2025. doi: https://doi.org/10.1007/s40819-025-01890-1

[46] M. A. Miller and C. K. Shahab, "REVIEW OF THE COST EFFECTIVENESS OF IMMUNISATION STRATEGIES FOR THE CONTROL OF EPIDEMIC MENINGOCOCCAL MENINGITIS," *Pharmacoeconomics*, vol. 23, pp. 333-343, 2005. doi: https://doi.org/10.2165/00019053-200523040-00004

[47] F. Brauer, *et al.*, "MATHEMATICAL MODELS IN EPIDEMIOLOGY, VOLUME 32," Springer, 2019. doi: https://doi.org/10.1007/978-1-4939-9828-9

[48] M. J. Keeling and P. Rohani, *MODELING INFECTIOUS DISEASES IN HUMANS AND ANIMALS,* Modeling Infectious Diseases in Humans and Animals, Princeton: Princeton University Press, 2018.

[49] S. Mandal, *et al.*, "PRUDENT PUBLIC HEALTH INTERVENTION STRATEGIES TO CONTROL THE CORONAVIRUS DISEASE 2019 TRANSMISSION IN INDIA: A MATHEMATICAL MODEL-BASED APPROACH," *Indian Journal of Medical Research*, vol. 151, no. 2-3, pp. 190-199, 2020. doi: https://doi.org/10.4103/ijmr.IJMR_504_20

[50] I. M. E. Lmojtaba and S. O. Adam, "A MATHEMATICAL MODEL FOR MENINGITIS DISEASE.," *Red Sea University Journal of Basic and Applied Science*, vol. 2, no. 2, p. 467–472, 2017.

[51] H. Christensen, M. Hickman, W. J. Edmunds, and C. L. Trotter, "INTRODUCING VACCINATION AGAINST SEROGROUP B MENINGOCOCCAL DISEASE: AN ECONOMIC AND MATHEMATICAL MODELLING STUDY OF POTENTIAL IMPACT," *Vaccine*, vol. 31, no. 23, p. 2638–2646, 2013. doi: https://doi.org/10.1016/j.vaccine.2013.03.034

[52] Y. Deng and Y. Zhao, "MATHEMATICAL MODELING FOR COVID-19 WITH FOCUS ON INTERVENTION STRATEGIES AND COST-EFFECTIVENESS ANALYSIS," *Nonlinear Dynamics*, vol. 110, no. 4, p. 3893–3919, 2022. doi: https://doi.org/10.1007/s11071-022-07777-w

[53] A. S. Afolabi and M. Miswanto, "MATHEMATICAL MODELING, OPTIMAL CONTROL AND COST-EFFECTIVENESS ANALYSIS OF DIPHTHERIA TRANSMISSION DYNAMICS," *Jambura Journal of Biomathematics (JJBM)*, vol. 6, no. 2, p. 88–108, 2025. doi: https://doi.org/10.37905/jjbm.v6i2.30851

[54] P. De Wals, L. Coudeville, P. Trottier, C. Chevat, L. J. Erickson, and V. H. Nguyen, "VACCINATING ADOLESCENTS AGAINST MENINGOCOCCAL DISEASE IN CANADA: A COST-EFFECTIVENESS ANALYSIS," *Vaccine*, vol. 25, no. 29, p. 5433–5440, 2007. doi: https://doi.org/10.1016/j.vaccine.2007.04.071

[55] M. A. Kuddus, A. K. Paul, and T. Theparod, "COST-EFFECTIVENESS ANALYSIS OF COVID-19 INTERVENTION POLICIES USING A MATHEMATICAL MODEL: AN OPTIMAL CONTROL APPROACH," *Scientific Reports*, vol. 14, no. 1, p. 494, 2024. doi: https://doi.org/10.1038/s41598-023-50799-6

[56] S. Olaniyi, O. S. Obabiyi, K. O. Okosun, A.T. Oladipo, and S. O. Adewale, "MATHEMATICAL MODELLING AND OPTIMAL COST-EFFECTIVE CONTROL OF COVID-19 TRANSMISSION DYNAMICS," *The European Physical Journal Plus*, vol. 135, no. 11, p. 938, 2020. doi: https://doi.org/10.1140/epjp/s13360-020-00954-z

[57] E. Vynnycky and R. White, *AN INTRODUCTION TO INFECTIOUS DISEASE MODELLING*, Oxford university press, 2010.

[58] C. W. Chukwu, *et al.*, "A MATHEMATICAL MODEL FOR CO-DYNAMICS OF LISTERIOSIS AND BACTERIAL MENINGITIS DISEASES," *Commun. Math. Biol. Neurosci*, vol. 2020, no. Article–ID, 2020.

[59] E. N. Wiah and I. A. Adetunde, "A MATHEMATICAL MODEL OF CEREBROSPINAL MENINGITIS EPIDEMIC: A CASE STUDY FOR JIRAPA DISTRICT, GHANA," *CURRENT APPLIED SCIENCE AND TECHNOLOGY*, vol. 10, no. 2, pp. 63-73, 2010.

[60] G. T. Tilahun, "OPTIMAL CONTROL ANALYSIS OF PNEUMONIA AND MENINGITIS COINFECTION," *2658971*, vol. 2019, no. 1, p. 2658971, 2019. doi: https://doi.org/10.1155/2019/2658971

[61] Z. Islam, *et al.*, "DEVELOPING A MATHEMATICAL MODEL FOR OPTIMAL COST-EFFECTIVE TREATMENT STRATEGIES APPLIED TO A DIPHTHERIA OUTBREAK," 2020.